Continental Shelf Research 285 (2025) 105372

Contents lists available at ScienceDirect

Continental Shelf Research

journal homepage: www.elsevier.com/locate/csr

Bottom depth carving the pelagic spatial organisation in large marine ecosystem: The case of North West Africa

Anne Mouget [a,b,*], Patrice Brehmer [c], Mohamed Ahmed Jeyid [d], Yannick Perrot [b], Ndague Diogoul [c,g], Momodou Sidibeh [e], Kamel Mamza [f], Anthony Acou [h], Abdoulaye Sarré [g]

[a] UMR BOREA Biologie des Organismes et Ecosystèmes Aquatiques, MNHN, CNRS, SU, IRD, UCN, UA, Station Marine de Dinard, CRESCO, 35800, Dinard, France
[b] Institut de recherche pour le développement, IRD, Lemar, DR ouest, Plouzané, France
[c] IRD, Univ Brest, CNRS, Ifremer, Lemar, CSRP, SRFC, Dakar, Senegal
[d] Institut Mauritanien de Recherche Océanographique et des Pêches, IMROP, BP 22, Nouadhibou, Mauritania
[e] The Fisheries Department, FD, 6 marina parade, Banjul, The Gambia
[f] Institut National de Recherche Halieutique, INRH, Casablanca, Morocco
[g] Institut Sénégalais de Recherche Agricole, ISRA, Centre de Recherche Océanographique de Dakar Thiaroye, CRODT, Pôle de recherche de Hann, Dakar, Senegal
[h] UAR Patrimoine Naturel – OFB, CNRS, MNHN – Station Marine de Dinard, CRESCO, 38 rue de Port Blanc, Dinard, France

ARTICLE INFO

Keywords:
Sound scattering layer
Bathymetry
Diel vertical migration
Pelagic structuration
Interannual trends

ABSTRACT

This study aimed to examine the spatial organization of pelagic communities within the water column along a horizontal gradient extending from the coast to the offshore area, categorized into three zones: inshore, offshore, and transition. Using fisheries acoustics, a total of 29 000 nautical miles of acoustic transects collected during 14 annual standardized surveys were analyzed using two complementary acoustic methods: (i) extraction of sound scattering layers (SSL) and (ii) echointegration (EI) across the entire water column, both horizontally and vertically averaged. The results revealed significant differences between the three bathymetric areas based on SSL and EI descriptors, with micro-nektonic communities in the transition area exhibiting intermediate characteristics between those in the inshore and offshore areas. The relative abundance of micro-nektonic communities decreased from shallow coastal areas to deep offshore areas, with a mean S_v from echointegration of −66.43, −74.39 and −73.65 dB for inshore, transition and offshore, respectively. The inshore area is different from the transition and offshore areas, which is confirmed by diel vertical migration (DVM) analyze through vertical profiles. All areas exhibited classic DVM type I; however, offshore and transition areas also presented unexpected DVMs of type II, *i.e.*, organisms descend deeper during the night, displaying distinct vertical profiles compared to the inshore area. This suggests that the functional and specific composition of pelagic micro-nektonic communities differed between inshore and offshore areas, indicating that organisms adjust their responses to their environment. Over two decades, the three bathymetric areas showed a significant increase in pelagic relative biomass and variation in SSL spatial structure. The number of SSLs significantly increase, from 0.97 to 1.05 inshore, from 1.75 to 2.25 in the transition area and from 2.2 to 2.7 offshore. Nevertheless, micro-nektonic communities reacted differently to interannual changes depending on the bathymetric areas, such as the minimal depth of the shallowest SSL. Fluctuations in SSL descriptors were highlighted over the study period, which may be related to multi-decadal oscillations in the Atlantic Ocean.

1. Introduction

Bathymetry is recognized as a structuring environmental factor for fish (Louisy, 2015), and phytoplankton (Huan et al., 2022) communities and is utilized in various models (Hedger et al., 2004; Kaschner et al., 2006; Lenoir et al., 2011). Marine organisms are constrained by bathymetry, but they also follow patterns that exhibit temporal fluctuations according to diel vertical migration (DVM), interannual variations (Lenoir et al., 2011), and long-term trends (Beaugrand et al., 2000; Brunel and Boucher, 2007).

* Corresponding author. UMR BOREA Biologie des Organismes et Ecosystèmes Aquatiques, MNHN, CNRS, SU, IRD, UCN, UA, Station Marine de Dinard, CRESCO, 35800, Dinard, France.
E-mail address: Anne.Mouget@mnhn.fr (A. Mouget).

https://doi.org/10.1016/j.csr.2024.105372
Received 2 February 2024; Received in revised form 23 October 2024; Accepted 24 November 2024
Available online 27 November 2024

While bathymetry plays a key role in structuring pelagic communities, biotic and abiotic factors also significantly influences their spatial distribution. Among abiotic factors, temperature is a key driver, affecting metabolic rates, growth, and reproduction of organisms, thereby shaping their distribution patterns (Bertrand et al., 2000; Hazen and Johnston, 2010; Netburn and Koslow, 2015). Dissolved oxygen concentrations are critical, especially in deeper waters or highly productive areas where oxygen minimum zones can develop, limiting the vertical distribution of many organisms (Bianchi et al., 2013a; Netburn and Koslow, 2015). Light penetration influences the depth of the photic zone, directly affecting primary productivity and the behavior of visual predators and their prey (Aksnes et al., 2017). Ocean currents play a vital role in the horizontal and vertical distribution of pelagic organisms, influencing larval dispersal, nutrient transport, and the formation of productive frontal zones (Bakun, 2006). Among biotic factors, primary productivity is fundamental, forming the base of the pelagic food web and attracting higher trophic level. In the southern CCLME, Diogoul et al. (2021, 2020) demonstrated that environmental parameters such as sea surface temperature, chlorophyll-a concentration, and wind-induced turbulence significantly influence the structure and distribution of SSLs.

The Canary Current Large Marine Ecosystem (CCLME) is situated along the West African coasts from 10°N to 40°N (Spall, 1990). Economically important for countries (Diankha et al., 2017; Görlitz and Interwies, 2013; Sarré et al., 2018), the CCLME's functioning is quite complex, depending on depth, latitude, coast specificity, and upwelling events (Diogoul et al., 2021). Previous studies on the CCLME (Arístegui et al., 2009; Auger et al., 2016; Barton et al., 1998) do not highlight the effect of upwelling and other environmental aspects on pelagic organism spatial structuration. Bottom depth is an environmental variable that well explains marine community structure (Majewski et al., 2017). The way depth controls the spatio-temporal organization of pelagic communities over the continental shelf remains poorly understood.

The most common method to describe the spatial organization of micro-nektonic communities in the marine environment is based on acoustic surveys (Brehmer et al., 2019; Simmonds and MacLennan, 2005), which are non-invasive and non-destructive for ecosystems (Brehmer, 2006). In this study, we used 14 acoustic sea surveys carried out over 21 years. Such a long-term dataset allowed us to study inter-annual variability and gain potential first insights into climate change effects. To analyze the organization of aggregating pelagic organism communities, we used Sound Scattering Layers (SSL) descriptors (Mouget et al., 2022). SSLs are aggregations of micro-nekton (organisms between 2 and 20 cm in length), macrozooplankton (organisms between 2 and 20 mm), and many other pelagic organisms, which play a key trophic role in pelagic ecosystems (Béhagle et al., 2017; Blanluet et al., 2019; Remond, 2015). SSLs are, therefore, structures that can be used as sentinel in marine ecosystems (Remond, 2015) as they are sensitive to spatial and long-term environmental changes (Hays et al., 2005).

SSLs have been extensively studied in different parts of the world. Methodologies have been developed to be adapted to different situations, from the deep ocean (Hersey et al., 1961) to inland waters (Jones and Xie, 1994), including reproductive and automatic methods (Cade and Benoit-Bird, 2014; Proud et al., 2015), on which we have based this study. The first related study on SSL in North West Africa dates back to 1988 (Schalk, 1988). Subsequent studies has been conducted over the years to follow (*e.g.* Champalbert et al., 2005; Diogoul et al., 2020; Sarré et al., 2018), focusing primarily on zooplankton (Diogoul et al., 2024) and small pelagic fish populations (Sarré et al., 2024).

SSLs are also used to understand patterns of organization, such as diel vertical migrations (DVM) (Benoit-Bird and Au, 2004) and monitor the ecological state of ecosystems (Diogoul et al., 2021). DVM is a daily movement of aquatic organisms that ascend to the surface at night and descend to deeper waters during the day to avoid predators and optimize food access (Brierley, 2014). The study of diel vertical migrations is essential for understanding marine ecosystem dynamics and the carbon cycle. These migrations influence trophic interactions (Guglielmo et al., 2011) and nutrient distribution by transporting biomass between deep and surface waters (Bianchi et al., 2013b). They also provide insight into species' behavioural adaptations and the impact of environmental changes, such as climate change (Hays et al., 2005). Some studies explored DVM in CCLME, such as Tiedemann and Brehmer (2017) or Mbaye et al. (2015).

Besides SSLs, echointegration-based descriptors (Perrot et al., 2018) collected from the water column are complementary thanks to the comprehensive scan of the water column realized by echo-integration, enabling the inclusion of organisms distributed outside the SSLs.

With our large spatial coverage and fine-resolution dataset, pelagic organism distribution patterns are compared between bathymetric areas and their inter-annual variability is analyzed. As fisheries acoustics are the most reliable (requiring low standardization) and available time series, particularly in poor data ecosystems, this study aims to evaluate, based on fisheries acoustics time series and without biological sampling, how bottom depth influences pelagic organization, considering independently three distinct areas commonly discriminated in fisheries sciences: the inshore, transition, and offshore areas.

2. Material and methods

2.1. Material

Acoustic data were collected using a 38 kHz transceiver type ES38-B on-board R/V Dr. Fridtjof Nansen with the following settings: at a depth of 5.5 m, an absorption coefficient of 8.7 dB km-1, a pulse length of 1.024 ms, and a maximum transmission power of 2000 W (Krakstad et al., 2006; Sarré et al., 2018). The echosounder was annually calibrated following the classic calibration procedure (Foote et al., 1987) using a standard copper sphere for 38 kHz. Data were recorded over the Canary Current Large Marine Ecosystem (CCLME).

The CCLME is one of the 64 large marine ecosystems (LMEs) defined worldwide to propose ecologically rational units of ocean space (Sherman, 1994). While the CCLME presents a global homogeneity, two areas, the North and South CCLME, can be discriminated against with either permanent or seasonal upwelling, respectively (Barton et al., 2013; Benazzouz et al., 2014). Seasonal upwelling occurs during the summer in the South CCLME (Benazzouz et al., 2014), and permanent upwelling occurs in the North part. To work on a homogeneous ecosystem, we reduce the dataset to the South part of CCLME without upwelling impact. CCLME is highly productive and allows the study of pelagic spatial structuration, mainly due to small pelagic fish and zooplankton. However, this area exhibits a wide range of environmental conditions influenced by currents (Faye et al., 2015), as well as local factors such as river plumes and coastal influences, impacting crucial parameters like sea temperature and macronutrient concentrations.

Hereafter we referred to the South part of CCLME as "SCCLME." The study area extended from the southern border of Senegal (12.15°N) to Cape Blanc (20.77°N) and from longitude 16°W to 18°W (Fig. 1).

To focus on the influence of bathymetry on the acoustic signal without interfered from upwelling regimes, our study area was limited to the SCCLME outside the permanent upwelling (Gómez-Letona et al., 2017). All surveys included in this study were conducted during the wet season (November and December) between 1995 and 2015, totalling 29 586 nautical miles (nmi) analyzed. The survey designs remained consistent over the years (Fig. 2), even if there is sometimes annual specificity. In particular, in 1995, offshore was only slightly covered by sampling. Surveys were conducted 24/24, covering day, night, and transitional periods. Transitional periods were defined using sun altitude, calculated based on date, time, and geographic position. Diel transition periods corresponding to sunset and sunrise, with a sun altitude between −18° and +18° (Lehodey et al., 2015; Perrot et al., 2018), were excluded from analyses to avoid density change bias due to diel vertical migrations (DVM). After recording, acoustic data were converted to the international hydro-acoustic data format HAC using the

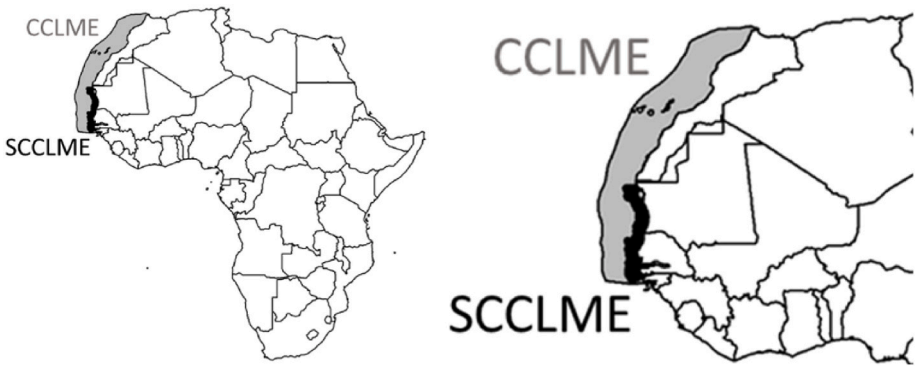

Fig. 1. Map of the Canary current large marine ecosystem (CCLME in grey) in the African Topical Atlantic Ocean, including the study area, named here the South part of the CCLME (SCCLME in black: Mauritania, Senegal and The Gambia).

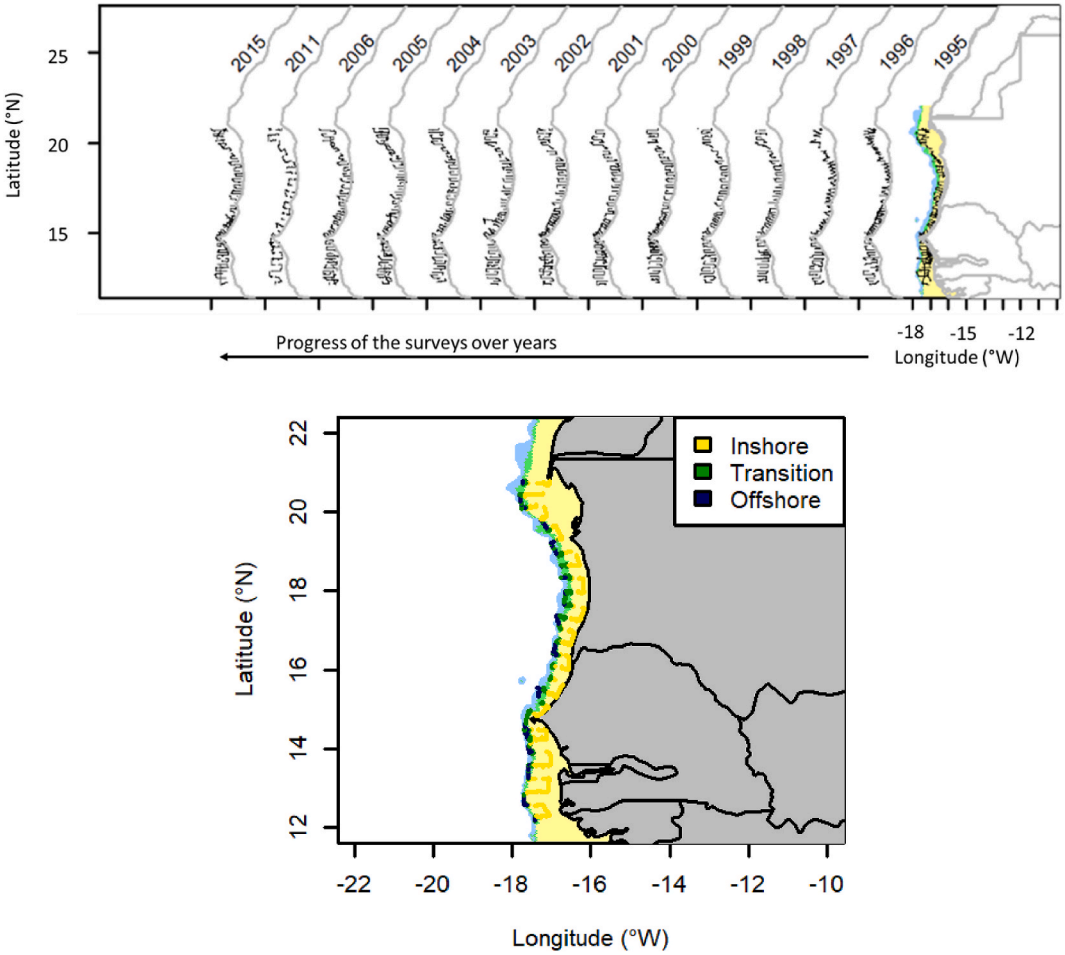

Fig. 2. a) Map of the acoustic survey sampling per year and bathymetry along the African coast (Mauritania, Senegal, and Gambia) in the Canary Current Large Marine Ecosystem. b) Zoom on an acoustic survey carried out in 2011. The acoustic sampling design is drawn in black along the coastline in grey. The continental shelf bathymetry is presented using a colour scale: In yellow, inshore (bottom depth <150 m); in green, transition (bottom depth in 150–500 m); and in blue, offshore (bottom depth >500 m).

Matecho algorithm (Perrot et al., 2018). Echograms have been cleaned using automatic filters based on Movies-3D software (Ifremer, 2024) Four filters have been applied: 1/unparasite to remove interference; 2/noise reduction (De Robertis and Higginbottom, 2007); 3/blank ping removal; 4/deep spike removal. The first 10 m have also been removed to avoid blind area and surface noise. All echograms have been manually checked to avoid mistakes.

The data were categorized into three bathymetric areas: inshore, transition, and offshore. The bottom depth was defined using acoustic data. The bottom depth has been estimated using the software Matecho using a backstep minimum level of −50 dB and then manually post-processed to correct bottom-line errors. Inshore corresponds to the shelf, close to the coasts, with a depth under 150 m. The transition includes bottom depths between 150 and 500 m, encompassing a deeper continental shelf and the slope. Offshore areas were defined as having bottom depths ranging from 500 to 1500 m. This zonation is commonly

used in studies, aligning with physical and biological functioning (*e.g.*, Gibson et al., 2005; Castillo et al., 2017). Fisheries acoustics data were clustered into elementary sampling units (ESUs) of 0.1 nautical miles (nmi) (Table 1).

2.2. Methods

The dataset was analyzed using two methods: (i) horizontally or vertically averaged echointegrated echograms and (ii) extracted Sound Scattering Layers (SSLs). Echointegration was conducted using a threshold of −100 dB to include everything in the water column. SSLs were extracted using Matecho (Perrot et al., 2018) from echointegrated echograms using a segmentation algorithm at an echo level threshold of −70 dB re 1 m^{-1}, denoted as dB hereafter. The −70 dB threshold was chosen to encompass both the micro-nektonic layers (Béhagle et al., 2016) and the contribution of pelagic fish. SSL descriptors were computed per ESU of 0.1 nmi to characterize SSLs in the water column up to a depth of 500 m. The maximal depth registered during surveys was 2500 m but with only a few values over 1000 m. The third quartile of the depth range over surveys is 160 m. Matecho computed six descriptors per ESU for each SSL.

Descriptors were selected to facilitate efficient analysis for comparing ecosystems at different depths and were based on the shallowest SSL and all SSLs (Mouget et al., 2022). The shallowest SSL, which is the SSL located closest to the surface, is the most independent SSL of the bottom depth, *i.e.*, it is the farthest from the bottom. This shallowest SSL is called SSL_1. Moreover, Mouget et al. (2022) highlighted that there were few ESUs with more than one SSL over the shelf. In addition to the shallowest SSL analysis, descriptors based on the entire water column or all SSLs were also used and added to the SSL descriptors (Table 2): (i) the mean volume backscattering strength (S_v in dB) from echointegrated echograms ($S_{v,\ EI}$) allowing an analysis of the whole water column; (ii) the S_v of shallowest SSL ($S_{v,\ 1}$) to analyze the acoustic importance of the shallowest SSL; (iii) the mean S_v of all SSLs ($S_{v,\ all}$) to have a complete view on all SSL along the water column; (iv) the minimal depth of the shallowest SSL ($đ_1$); (v) the width of shallowest SSL ($\dot{W}_1$) to identify the behaviour of shallowest SSL; (vi) the number of SSLs (Ɗ) on the organisation of the water column. $S_{v,\ EI}$, $S_{v,\ 1}$, $S_{v,\ all}$, $đ_1$, $\dot{W}_1$, and Ɗ are referred to as descriptors from here. S_v (dB) serves as a proxy for pelagic biomass (Ariza et al., 2022; Holland et al., 2021), hereafter referred to as pelagic biomass.

The dataset's spatial auto-correlation along transects was considered negligible (Béhagle et al., 2014; Domokos, 2009; Sabarros et al., 2009). Statistical analyses were conducted using R version 4.3.2 (R Core Team, 2021).

Kernel density was computed for each SSL descriptor ($S_{v,\ 1}$, $S_{v,\ all}$, $đ_1$, $\dot{W}_1$) and echointegration descriptor ($S_{v,\ EI}$). Kernel density estimation (Sheather and Jones, 1991; Zhang et al., 2018) was employed to construct probability density functions. To compare the densities from descriptors and variations of $S_{v,EI}$ with respect to depth, two tests were used. The Wilcoxon test compared means (Fay and Proschan, 2010), while Spearman's rank correlation test estimated the degree of correlation between two curves (Croux and Dehon, 2010). For discrete descriptors, *i.e.*, the number of SSLs (Ɗ), the Chi-square test was employed (McHugh, 2013). All statistical tests were conducted with a significance threshold of 0.05 for the *p*-values. The analysis of different acoustic descriptors allowed the examination of the relative importance of acoustic density within and outside of SSLs, as well as the difference between the shallowest and all SSLs, highlighting variations in water column organizations.

Vertical profiles were computed using the complete dataset of S_v from echointegration, consisting of data for each cell of one ESU length (0.1 nmi) by 1-m depth. For each year, a vertical profile was computed as the mean of all data at each depth with an accuracy of 1 m depth. When there were fewer than 50 ESUs, no mean was computed to avoid unreliable outliers. Vertical profiles for each year were then averaged to produce a single curve for each depth category (inshore, transition, offshore). To compare patterns of vertical profiles, the datasets were truncated to the length of the smallest profile, *i.e.*, the length of the shelf profile, up to 150 m. Correlations between curves were calculated using the Spearman correlation coefficient (Kendall, 1938). The mean difference between the two curves was determined by averaging the differences at each point.

To assess the relative importance of acoustic classes in inshore, transition, and offshore areas, another analysis was performed. For each survey, each cell of 1 ESU length by 1-m width was assigned to one of four $S_{v,\ EI}$ classes based on S_v values between arbitrary limits of ten dB intervals: [−50; −60[, [−60; −70[, [−70; −80[, [−80; −90[dB as defined by Mouget et al. (2022). Cells with values outside were excluded. The relative importance of each class was then calculated per bathymetric area by dividing the number of cells in an $S_{v,\ EI}$ class by the number of classified cells in the corresponding ESU.

To perform DVM analysis, densities of $S_{v,\ EI}$, $S_{v,\ 1}$, and $S_{v,\ all}$ were computed using the Kernel density method (Sheather and Jones, 1991; Silverman, 1986) for each bathymetric area separately during the day and night periods. The day density was then subtracted from the night density to obtain a single differential curve for each inshore, transition, and offshore area. The curves were analyzed using the same method as vertical profiles.

To analyze changes over decades and inter-annual changes, linear regressions and polynomial regressions of orders 2 and 3 were calculated using years as the single explicative variable (Mouget et al., 2022). The linear regression (first order) follows the form $y = ax + b$, while the second-order polynomial regression takes the form $y = ax^2+bx + c$, and the third-order polynomial regression is expressed as $y = ax^3+bx^2+cx + d$. The year is treated as a continuous variable since surveys were conducted during the same months each year.

Table 1
Summary of the dataset collected during sea surveys onboard the R/V Dr Fridtjof Nansen over the South part of the Canary Current Large Marine Ecosystem between 1995 and 2015. The number of Elementary Sampling Units (ESU) of 0.1 nautical miles (n = 295 860) are detailed for inshore (bottom depth <150 m), transition (bottom depth from 150 to 200 m), and offshore (bottom depth >500 m) areas.

Year	Number of ESUs (0.1 nmi)			
	Inshore	Transition	Offshore	Total
1995	19 636	4514	9	24 159
1996	17 663	3107	1303	22 073
1997	15 338	2044	1186	18 568
1998	16 093	2479	1695	20 267
1999	12 597	2858	2286	17 741
2000	16 385	3590	2379	22 354
2001	15 451	2323	4557	22 331
2002	17 757	6401	475	24 633
2003	16 251	2620	3275	22 146
2004	15 253	2745	2699	20 697
2005	18 546	2292	2651	23 489
2006	14 971	3196	2431	20 598
2011	8383	4077	2501	14 961
2015	15 666	5531	943	22 140
Total	219 990	47 480	28 390	295 860

3. Results

3.1. Comparison of SSL and echointegration descriptors by bathymetric areas

3.1.1. Comparison of descriptors

The Kernel density curves estimate the probability density function of the bathymetry. They smooth out the distribution of data points to create a curve that represents the density of data across a range, allowing for comparison of distributions.

Table 2
Descriptors used in this study, their symbols, units, formulas, and or reference(s). S_v is the volume backscattering coefficient in dB, and s_v is the volume backscattering coefficient in m^{-1} (*MacLennan* et al., *2002*). N/A means not applicable. "i" is the sound scattering layers (SSL) number, starting at 1 for uppers SSL in surface, and "j" is the Elementary Sampling Unit (ESU) number.

Denomination of descriptors	Symbol	Unit	Formulae	Reference(s)
Bottom depth at ESU j	D_j	Meter (m)	N/A	–
Number of echointegrated cells at ESU j	N_j	–	N/A	–
Number of SSL at ESU j	$Ð_j$	–	N/A	Urmy et al. (2012); Weill et al. (1993); Woillez et al. (2007)
Mean S_v from echointegrated echograms at ESU j	$S_{v,\ EI,\ j}$	Decibel (dB)	$10\ \log_{10}\frac{\sum_{i=1}^{N} 10^{S_{v,EI,i,j}/10}}{N}$	MacLennan et al. (2002)
S_v of shallowest SSL at ESU j	$S_{v,\ 1,\ j}$	Decibel (dB)	$10\log_{10}s_v$	Mouget et al. (2022 adapted from MacLennan et al. (2002)
Mean S_v of all SSLs at ESU j	$S_{v,\ all,\ j}$	Decibel (dB)	$10\ \log_{10}\frac{\sum_{i=1}^{Ð} 10^{S_{v,i,j}/10}}{Ð}$	Mouget et al. (2022) adapted from MacLennan et al. (2002)
Minimal depth shallowest SSL at ESU j	$đ_{1,\ j}$	Meter (m)	N/A	Mouget et al. (2022)
Width of shallowest SSL at ESU j	$Ẇ_{1,\ j}$	Meter (m)	N/A	Mouget et al. (2022)

The density curves (Fig. 3a, b, c) exhibited distinct patterns for all acoustic ($S_{v,\ EI}$, $S_{v,\ 1}$, $S_{v,\ all}$) across the three bathymetric areas. Inshore had maxima for higher values of S_v than transition and offshore. The inshore's maxima were at −64.4, −63.5, and −63.7 dB for $S_{v,\ EI}$, $S_{v,\ 1}$, and $S_{v,\ all}$, respectively, while maxima for the offshore area shifted towards lower values with −74.0, −64.5, and −66.5 dB, respectively. Peaks of the transition area were close to offshore ones, with peaks at −73.9, −64.7, and −67.3 dB for $S_{v,\ EI}$, $S_{v,\ 1}$, and $S_{v,\ all}$, respectively. Although the correlation between the curves was not significant, all curves were single-modal. The shift between the inshore and other curves (transition and offshore) was more pronounced for $S_{v,\ EI}$, with a difference of almost 10 dB (−64.4 dB inshore *vs* −74.0 and −73.9 dB in transition and offshore, respectively).

For descriptors based on the shallowest SSL ($đ_1$ and $Ẇ_1$), transition and offshore presented similar curves. The inshore curve is similar but with a higher kernel density for inshore at the maxima. The curves were not significantly correlated. The number of SSLs (Ð) revealed two different spatial organizations. The first one occurred in transition and offshore areas and was characterized by an increase in the percentage of ESUs from zero to two SSLs (an increase from 2.8% (Ð = 0) to 35.4% (Ð = 2) and from 1.5% (Ð = 0) to 35.9% (Ð = 2) for transition and offshore, respectively). The second behaviour was observed only in the inshore, with an increase in the percentage of ESUs only up to one SSL. Inshore had 84.7% of ESUs with only one SSL, whereas ESUs from transition and offshore were more distributed between all numbers of SSLs (with a maximal percentage of 38.5% and 35.9% for transition and offshore, respectively).

3.1.2. Vertical profiles of $S_{v,\ EI}$

Vertical profile resumes the vertical structuration. For each depth, the mean has been calculated, using all acoustic data from echointegration of this depth in the bathymetric area.

The three vertical profiles of $S_{v,\ EI}$ exhibited similar patterns across all three bathymetric areas (Fig. 4). Correlation tests between the three profiles were significant, with a correlation coefficient greater than 0.95. However, inshore vertical profiles displayed higher $S_{v,\ EI}$ values from the surface to 100 m depth. The mean difference between inshore and transition profiles was 2.4 dB for depths up to 150 m and 2.6 dB for depths up to 150m between inshore and offshore profiles. The mean difference between transition and offshore was 0.18 dB for depths up to 100 m and 0.93 dB for depths up to 500 m. Additionally, we observed that the S_v values were higher in the offshore area than in transition areas up to a depth of 200 m depth, after which the transition area exhibited higher values of S_v.

3.2. Comparison of $S_{v,\ EI}$ classes per bathymetric areas

In this section, we compare the distribution of elementary sampling units (ESUs) based on Sv, EI, across different bathymetric areas. By examining these categories we highlight the distribution and relative abundance of SSL values across the three bathymetric zones, offering insight into spatial variability in sound scattering across different depth zones.

The comparison of the relative importance of $S_{v,\ EI}$ classes across different depth categories revealed interesting patterns across the three bathymetric areas (Fig. 5). Inshore areas had a higher proportion of the class [−60; −50[(11.6%) compared to transition (3.8%) and offshore areas (2.3%). Conversely, the $S_{v,\ EI}$ classes [−80; −70[and [−90; −80[dB were more abundant in transition (47.9% and 20.0%, respectively) and offshore areas (52.5% and 15.6%, respectively) compared to inshore (35.5% and 10.8%, respectively). The class [−70; −60[dB was the most abundant in all areas, with inshore (40%) having the highest proportion and transition and offshore (46 and 51%, respectively) having the highest proportion for [−80; −70[dB. The similarities between transition and offshore areas were evident, especially for the lower proportion of the class [−70; −60[dB (28.3 and 29.6%, respectively) compared to inshore (42.2%). These proportions were significantly independent of the three bathymetric areas, even though transition and offshore showed similar distributions.

3.3. Comparison of DVM per bathymetric areas

3.3.1. Diel vertical migration through comparison of descriptors

The differences between night and day density curves across the three bathymetric areas (inshore, transition, and offshore), are compared based on all surveys conducted between 1995 and 2015, focusing on various sound scattering layer (SSL) parameters. This comparison helps reveal the diurnal variability in SSL across the different depth zones.

Mean S_v ($S_{v,\ EI}$) exhibited different patterns according to the bathymetric area considered. The patterns were similar in inshore and transition areas (significant Spearman coefficient of 0.91) (Fig. 6a). They both had a peak with negative values of density difference (−0.032 at −72 dB and −0.022 at −78 dB, for inshore and transition areas, respectively) followed by a positive peak. The offshore curve had a different shape, with two negative and two positive peaks.

The DVMs of the shallowest SSL, $S_{v,\ 1}$, varied according to similar patterns, whatever the bathymetric area (Fig. 6b). However, the lowest DVM values were observed for inshore areas than for both offshore and transition areas.

The DVMs of all S_v SSLs ($S_{v,\ all}$, Fig. 6c) showed similar patterns to the shallowest SSLs ($S_{v,\ 1}$, Fig. 6b). Indeed, the DVMs shifted from negative to positive values at a threshold of 0.64 and peaked at −0.6 dB for $S_{v,\ all}$ = 68 dB, and peaked at +0.3 and + 0.2 for offshore and transitional areas, respectively. Noteworthy, these DVMs were less marked than for shallowest SSLs.

The difference in the relative importance of $S_{v,\ EI}$ classes (Ð) between day and night was limited to 8% in transition and offshore areas, whatever the number of SSLs, whereas they were much higher inshore, where they reached up to 62% (Fig. 6d). This highlighted high changes

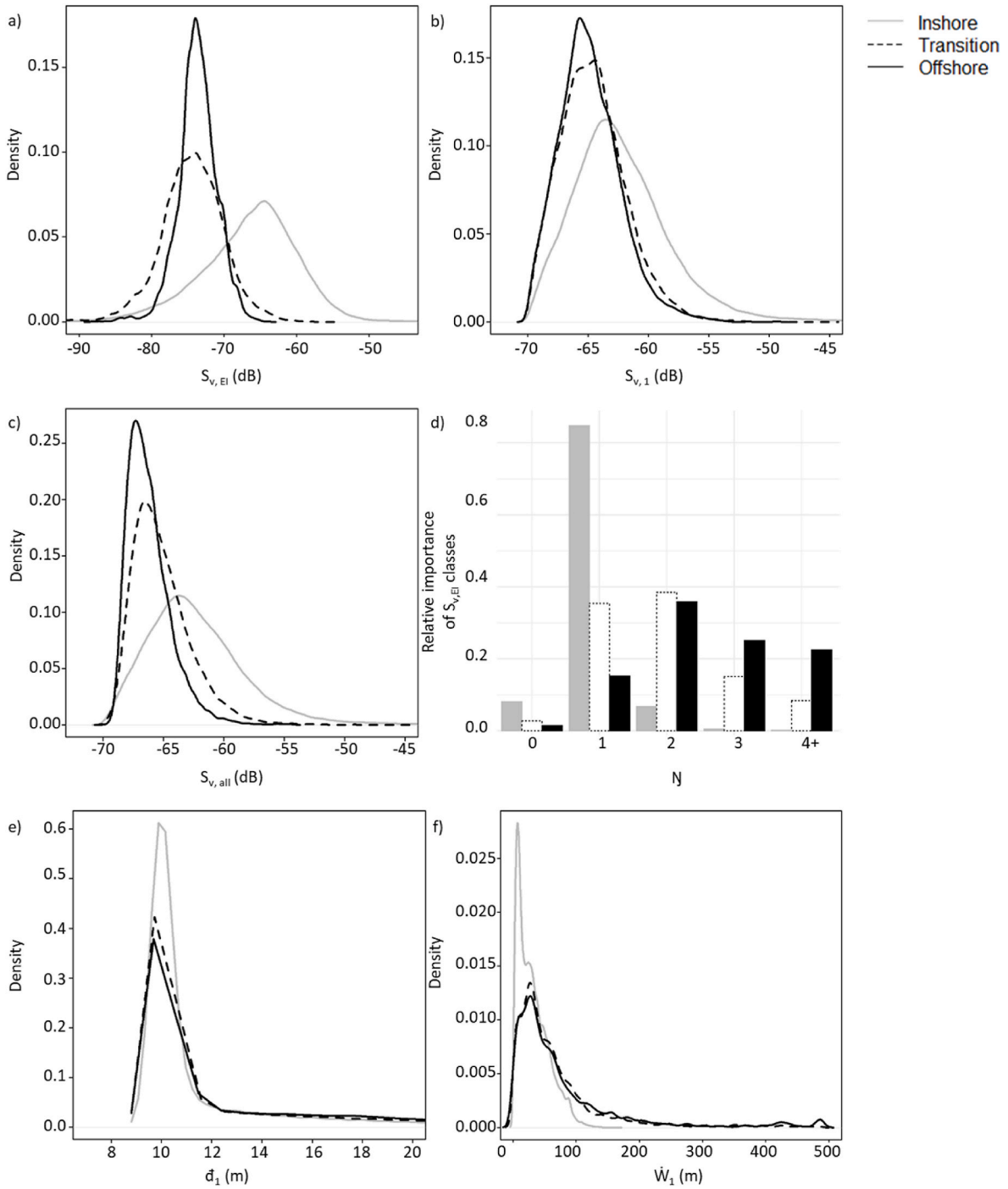

Fig. 3. Comparison of differences between Kernel density curves for the three bathymetric areas for all surveys analyzed (1995–2015). a) Mean volume back-scattering coefficient S_v (in dB) from echointegrated echograms ($S_{v, EI}$); b) S_v of shallowest sound scattering layer ($S_{v, 1}$); c) S_v of all sound scattering layers ($S_{v, all}$). The bathymetric areas are represented as follows. In full grey, the inshore (bottom depth <150 m). In dotted black, the transition (bottom depth in 150–500 m). In full black, the offshore (bottom depth >500 m). d) Relative importance of elementary sampling units (ESU) with 0, 1, 2, 3 or more (4+) number of sound scattering layers (Ŋ) by bathymetric area. The x-axis is the ratio for each $S_{v, EI}$ class. e) Minimal depth of shallowest sound scattering layer (đ$_1$). f) Width of shallowest sound scattering layer (Ẇ$_1$).

in the number of SSLs between day and night in the inshore area.

All density differences were positive or close to zero for đ$_1$, whatever the bathymetric area and the depth of the shallowest SSL (Fig. 6e). This indicates that minimum depths were shallower during nighttime than during daytime. For all bathymetric areas, the density difference decreased with the depth of the shallowest SSL. Interestingly, the highest differences were observed in the transition area, followed by offshore and inshore areas, suggesting that vertical movements have a higher amplitude in the transition area than both in offshore and inshore areas.

Differences in SSL widths (Ẇ$_1$, Fig. 6f) have similar patterns in transition and offshore, positive from 43 m width. This means that during the daytime, there were more SSLs with a width under 43 m than during nighttime. Therefore, SSL was thinner during the daytime. Inshore, the difference is positive from 10 m width. Therefore, the width of SSLs did not change between day and night for large SSLs (with a

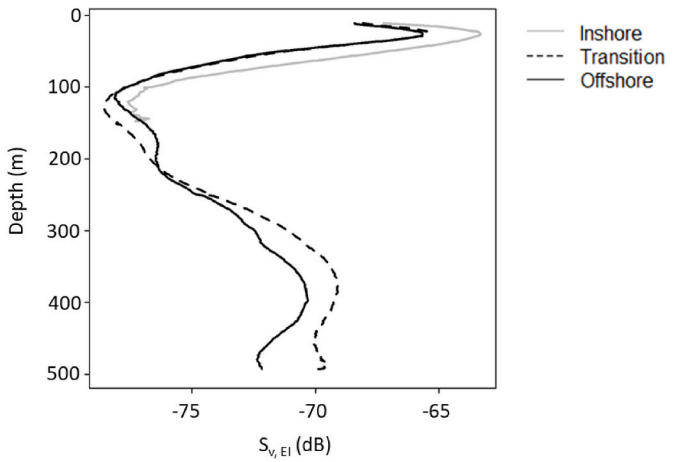

Fig. 4. a) Vertical profiles of mean S_v from echointegrated echograms ($S_{v, EI}$) of all survey years (0–500 m). In full grey, the inshore (bottom depth <150 m). In dotted black, the transition (bottom depth [150–500 m]). In full black, the offshore (bottom depth >500 m).

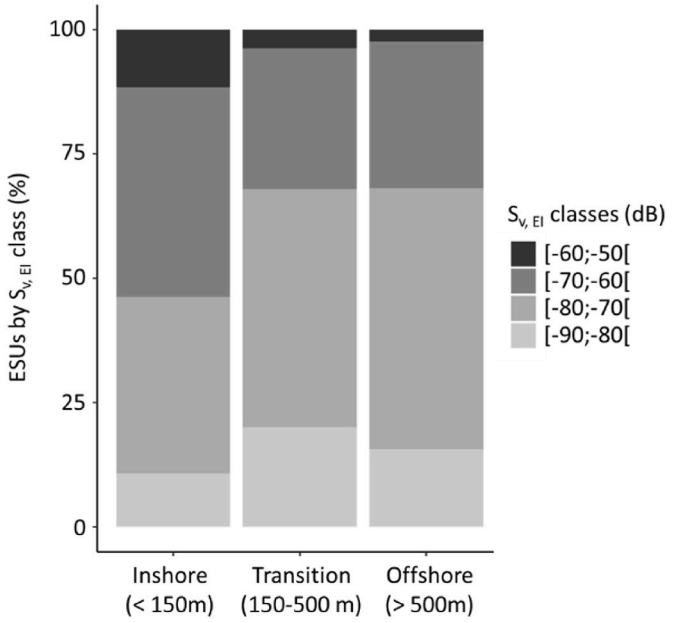

Fig. 5. Comparison of percentage of Elementary Sampling Unit (ESU of 0.1 nmi, n = 295 860) in each category of mean volume backscattering strength (S_v in dB) from echointegrated echograms ($S_{v, EI}$) for all surveys conducted from 1995 to 2015, across the inshore (depth <150 m), transition (depth in 150–500m) and offshore (depth >500 m) areas. The $S_{v, EI}$ classes are represented as follows: light grey: $S_{v, EI}$ class in the range [-90; −80[dB; in grey, [-80; −70[dB; in dark grey, [-70; −60[dB; and in black, [-60; −50[dB.

width over 10 m).

3.3.2. *Diel vertical migration through vertical profiles of $S_{v, EI}$*

The analysis of vertical profiles of $S_{v, EI}$ of DVM (Fig. 7ab) showed similar patterns between transition and offshore areas, with a strong significant correlation coefficient of 0.90 observed between the two profiles. In contrast, the vertical profile from the inshore area showed an inverse correlation to both transition and offshore areas. Notably, significant negative correlation coefficients of −0.53 and −0.77 were observed for transition and offshore areas, respectively.

All statistical tests, including DVM comparison, comparing eight descriptors in pairs between inshore, transition, and offshore, were computed, revealing 27 significant differences out of 45 tests conducted (Table 3). Thirteen tests analyzing the difference between day and night were significant out of 21 tests conducted. These tests also highlight the high correlation between transition and offshore for the shallowest SSL (with Spearman coefficient ranging from 0.78 to 0.90). When the entire water column was included ($S_{v, EI}$ and $S_{v, all}$), the correlation between transition and offshore was less important (0.56 and 0.48, respectively). DVM was significantly different inshore, with no correlation with other bathymetric areas.

3.4. *Inter-annual trend per bathymetric areas*

This section explores the temporal patterns of acoustic descriptors and the results of regression analysis for sound scattering layers (SSLs) across different bathymetric areas over two decades (1995–2015). Doing so we provide an overview of how these acoustic descriptors have changed over time across the inshore, transition, and offshore areas.

All indicators showed significant shifts between 1995 and 2015, following either linear trends or polynomial trends. Notably, the mean pelagic biomass ($S_{v, 1}$, $S_{v, all}$, and $S_{v, EI}$) significantly change over time in all areas. In the inshore area (Fig. 8a) $S_{v, EI}$ increased from −67.5 dB in 1995 to −66 dB in 2000, with a stagnation of values after. In the offshore and transition areas (Fig. 8b and c), the pelagic biomass showed a significant linear increase throughout the entire period, reaching maximum values of −72 and −74 dB in 2005 in the transition area and offshore, respectively. In the transition area, the last value (2015) is lower, which can suggest the start of a decrease in this area.

The shallowest SSL, as measured by $S_{v, 1}$, displayed distinct patterns depending on the area. In the inshore area, it followed a Gaussian-like curve with a peak in 2005 (Fig. 8d). No significant trend was observed in the transition areas (Fig. 8e). Offshore, $S_{v, 1}$ exhibited a hyperbolic trend with low values in 2005 and high values in 1995 and 2005 (Fig. 8e). In Fig. 8f and 2015 has similar values to 1995 and 1996, and the 4 previous surveys (2004, 2005, 2006, and 2011) had high values, which explains the shape of the regression.

The mean patterns of all SSL ($S_{v, all}$) mirrored the patterns of $S_{v, 1}$ for the inshore (Fig. 8g) and offshore (Fig. 8i) areas. However, in the transition area (Fig. 8h), the $S_{v, all}$ pattern resembled that of the inshore area, with a S_v peak observed in 2004–2005.

The number of SSLs (Ɒ) increased in all areas (Fig. 8j, k, l). Inshore, Ɒ showed a significant increase over time from 0.95 to 1.05 SSL (Fig. 8j; $R^2 = 2.35\ 10^{-3}$; slope = $3.77\ 10^{-3}$). Even without considering the highest Ɒ value of the time series (2015), the linear regression remained significant. In the transition area, Ɒ also exhibited a significant increase ($R^2 = 1.66\ 10^{-2}$; slope = $2.29.10^{-2}$) (Fig. 8j), while the linear trend in the offshore area was not significant, although an increase from 1995 to 2005 was observed, and reaching an asymptote. This curve follows a 3rd-order polynomial regression ($R^2 = 1.20\ 10^{-2}$).

The minimal depth of the shallowest SSL ($đ_1$) decreased over time in the inshore area (Fig. 8m) following a third-order pattern, while it remained relatively unchanged in the transition area (Fig. 8n) and increased offshore following a third-order pattern (Fig. 8o). Interestingly, a discrete hyperbolic pattern emerged in the inshore area, while a parabolic pattern was observed offshore. In both cases, a change in trend direction was again reported during the 2004–2006 period.

The width of the shallowest SSL, $\dot{W}_1$, significantly increased over time in transition and offshore areas. The width increased from 50 m to approximately 80 m (transition, Fig. 8q) and 120 m (offshore, Fig. 8r), with a first-order polynomial estimate of 235 ($R^2 = 9.71\ 10^{-4}$) and 3693 ($R^2 = 6.17\ 10^{-2}$) for transition and offshore area, respectively (Table 4). In the inshore area, the trend was not well-defined.

4. Discussion

The high number of ESUs processed in each bathymetric area enabled reliable comparisons. Few shallow coastal samplings have been

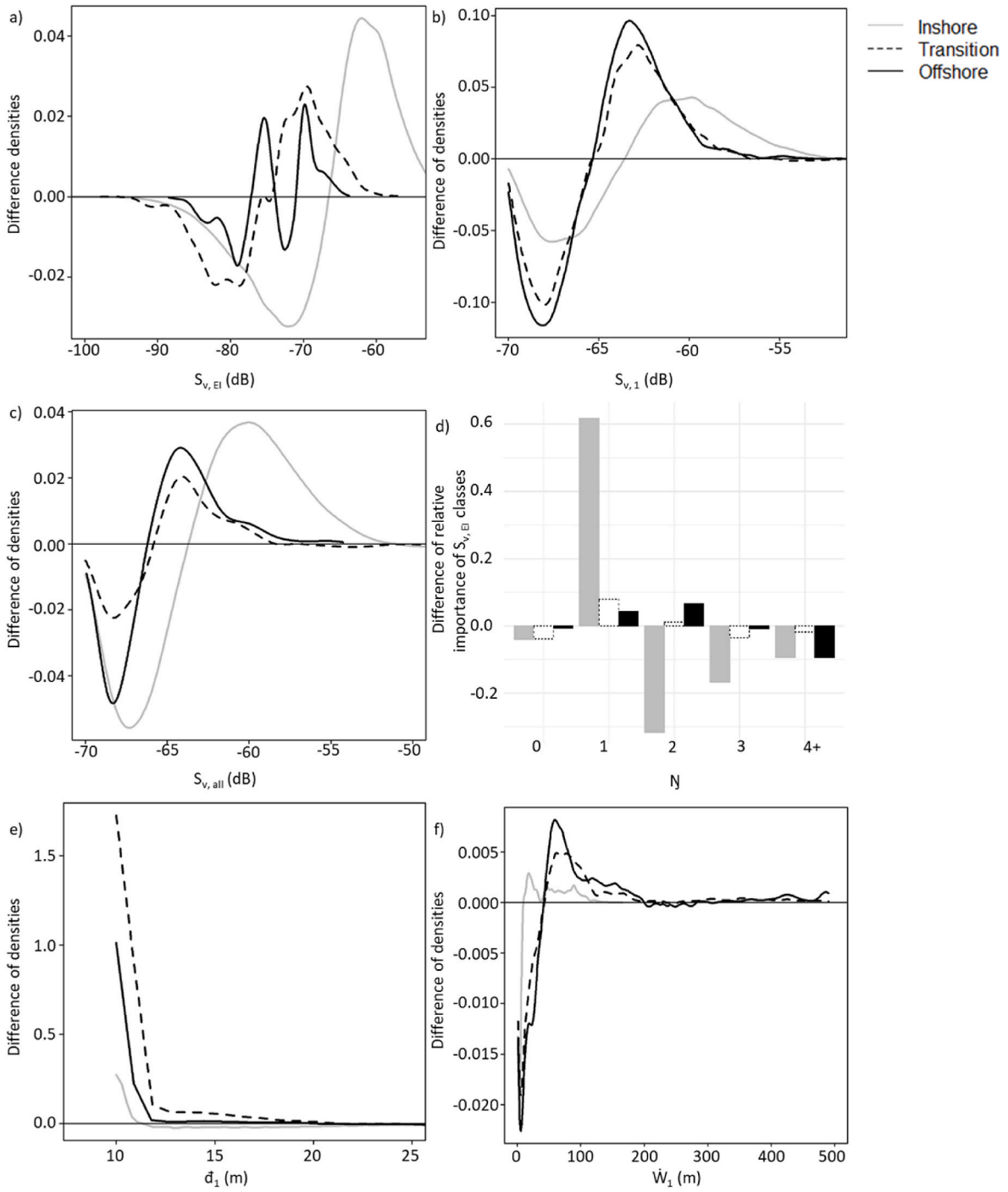

Fig. 6. Comparison of difference between density curve of night and day (all surveys 1995–2015) for the three bathymetric areas. In full grey, the inshore (depth <150 m); in dotted black, the transition (depth in 150–500 m); in plain black, the offshore area (depth >500 m). a) Mean S_v from echointegrated echograms ($S_{v, EI}$); b) S_v of shallowest sound scattering layer ($S_{v, 1}$); c) mean S_v of all sound scattering layers ($S_{v, all}$); (d) difference between relative number of SSLs (Ṇ) between nighttime and daytime; e) minimal depth of shallowest sound scattering layer ($đ_1$); f) width of shallowest sound scattering layer ($Ẇ_1$).

carried out, as is typical in fisheries acoustics surveys (Brehmer et al., 2006; David et al., 2024), for safe navigation.

In this study, all surveys have been conducted during the wet season, in October and/or November, which allow a certain homogeneity and exclude upwelling impact. However, the upwelling regime completely changes ecosystem functioning, with different physicochemical situations and high productivity, which impacts the whole ecosystem. Effectiveness of acoustics descriptors to assess pelagic community organisation.

The SSL descriptors (Mouget et al., 2022) appeared efficient for monitoring SSLs and micro-nektonic communities, highlighting differences and similarities within the SCCLME between the three studied bathymetric areas. Descriptors from echointegration were complementary to SSL ones. The indicators derived from echointegration ($S_{v, EI}$ by ESU, vertical profiles of $S_{v, EI}$, $S_{v, EI}$ classes) allowed exploration of the different acoustic communities according to their acoustic responses. $S_{v, EI}$ analysis was more exhaustive but required additional computational work, in contrast to SSL descriptors (Mouget et al., 2022), which could be used routinely to compare and monitor the nonspecific spatial organization of pelagic communities in marine ecosystems.

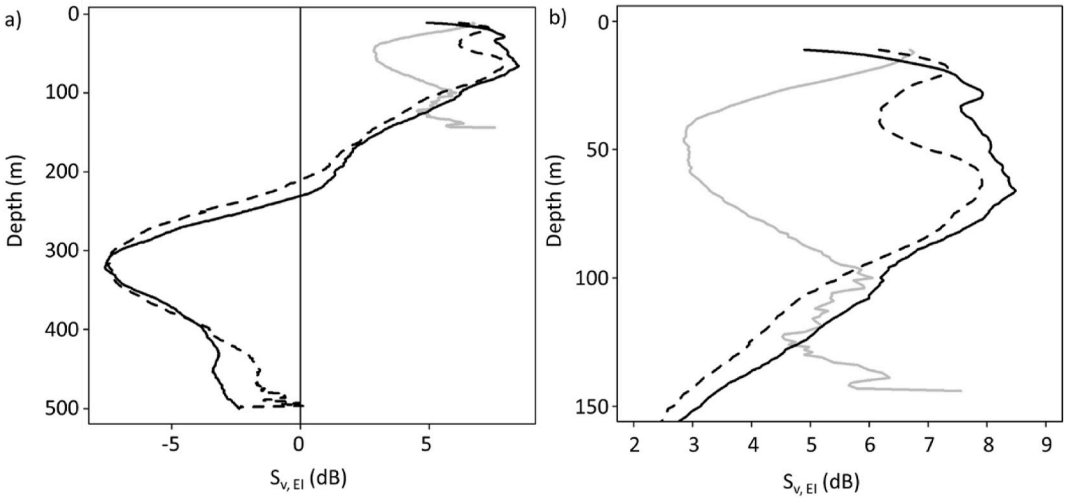

Fig. 7. Differential vertical profiles of mean volume backscattering strength (S_v in dB) from echointegrated echogram ($S_{v,\ EI}$) for all surveys (1995–2015). The profiles were obtained by subtracting night-time from daytime echograms for the following depth ranges: a) all depths (0–500 m). b) Zoom on 0–150 m depth. The bathymetric areas are indicated as follows: full grey, the inshore (bottom depth <150 m); in dotted black, transition (bottom depth in 150–500 m); in plain black, offshore (bottom depth >500 m).

4.1. Comparison of inshore, transition, and offshore pelagic areas using echointegration and SSL descriptors

The observed descriptors reveal significant distinctions in pelagic communities and their vertical distribution across the three bathymetric areas. Notably, pelagic biomass (S_v) is markedly higher in shallower waters, consistent with prior studies highlighting the increased abundance of pelagic fish (Brehmer et al., 2006; David et al., 2022) and plankton (Gasol et al., 1997) in coastal areas. These shallow waters, such as those inhabited by swimbladder fish species like *Clupea harengus* (Maravelias, 1999) and *Sardinella maderensis* (Sarré et al., 2018), serve as crucial spawning and nursery grounds, exhibiting a high abundance of ichthyoplankton (Tiedemann et al., 2017).

The vertical structuring of pelagic biomass in the water column is linked to the bathymetric area. Although vertical profiles from $S_{v,\ 1}$, $S_{v,\ all}$, and $S_{v,\ EI}$ exhibit peaks at similar values for transition and offshore, their amplitudes differ, while inshore demonstrates a peak for distinct pelagic biomass. As acoustic responses are species-dependent, inshore communities appear distinct from those in transition and offshore areas. Previous studies have validated the differentiation of communities along bathymetric gradients (Louisy, 2015; Smith and Brown, 2002), suggesting that the varied pelagic biomass (S_v) peaks along bathymetric areas correspond to different species assemblages with similar acoustic responses. The size of the water column, constrained by surface and bottom boundaries, significantly influences inshore areas compared to deeper regions. This constraint can explain the fact that the number of SSLs (Ɗ) exhibits a maximal ratio of ESUs for a single SSL, whereas transition and offshore are similar, with a majority of ESUs with two SSLs. However, some other pelagic organizations, such as $đ_1$ and $\dot{W}_1$ (minimal depth and width of the shallowest SSL), remain independent of the bathymetric area. This underscores that the shallowest SSL is constrained by environmental parameters, especially bathymetry (Marchal et al., 1993; Weston, 1958). The micro-nektonic organisms of the SSLs establish trophic relationships with primary producers; thus, the size of the SSL (height, surface) could be optimal depending on species organization or simply consistent across bathymetric constraints. The minimal depth of the shallowest SSL is constrained by the thermocline (Diogoul et al., 2020). A portion of SSL remains close to the surface (<50m) regardless of bathymetry, making them sensitive to ocean surface characteristics (Fig. S1).

Analysis of $S_{v,\ EI}$ vertical profiles confirms differences between inshore *vs.* offshore and transition. The similarity between transition and offshore is primarily observed in the upper part of the water column (0–100 m), indicating that a shallower micro-nektonic community is continuously present whatever the bathymetry. Deeper (>100m), the $S_{v,\ EI}$ of the transition area becomes progressively different from the offshore area with depth. Such difference could be attributed to change (s) in community and/or environment (Diogoul et al., 2020). Inshore $S_{v,\ EI}$ follows the same global pattern as others, albeit slightly shifted, with higher values of S_v. These elevated values could correspond to more pelagic fish, supporting the hypothesis of different species composition but similar organization due to environmental parameters, which vary based on the distance from the coast (Schickele et al., 2020).

Considering the entire water column, each depth category exhibits its predominant acoustic class ($S_{v,\ EI}$ classes). This result aligns with our findings on pelagic biomass (S_v) of SSLs, where transition and offshore areas are similar. They differ slightly for classes [−60; −50[and [−90; −80[dB, higher for the transition than offshore, possibly due to inshore contiguity with the transition area. The inshore area is characterized by a significant percentage of ESUs over −50 dB: classes [−60; −50[and [−70; −60[dB are highly represented inshore. Higher classes of S_v, [−70; −60[and [−60; −50[correspond to larger organisms such as pelagic fishes, while lower S_v values are indicative of zooplankton (Diogoul et al., 2021). A comparison of inshore and offshore areas highlights differences in fish species composition (Sarré et al., 2018). The acoustic profiles of the transition area are closer to offshore than those of inshore areas, especially the shallowest SSL. Species composition and DVMs are driven, among other environmental parameters, by bottom depth (Collins et al., 2012; Macpherson and Duarte, 1991), revealing structural differences between the three bathymetric areas, which necessitate separate considerations for modelling and monitoring. A modelling will be more accurate if only focused on a single bathymetric area, *i.e.*, we suggest separate models per area.

The delimitation between the transition and offshore areas can be further refined. We suggest developing an algorithm that takes into account other bathymetric factors, such as the slope, for future studies. We would like to improve our study by adding topometric measurement, as presented by Borland et al. (2021), which can be informative in understanding SSL distribution. Another way to develop is to include the ultra-shallow coastal (<10m depth) area, including the surf zone, which is not investigated in this study and should present some specific characteristics compared to the three bathymetric strata studied.

Table 3
Statistical analysis comparing descriptors (by pair) between inshore, transition, and offshore areas for a full diel cycle (global analyses) and the difference between daytime and nighttime (diel vertical migration analyses). Note: Wilcoxon and Spearman tests were conducted for continuous data, while the Chi-square test was used for discrete data (Ɒ and $S_{v,\ EI}$ classes). "ns" indicates non-significant results. "SSL" refers to the sound scattering layer.

Descriptor	Symbol	Compared bathymetric area	Wilcoxon test or chi-square *p*-value	Spearman coefficient
Global analyses (including day and night)				
Mean S_v from echointegrated echograms	$S_{v,\ EI}$	Inshore - transition	<0.05	0.97
		Transition - offshore	<0.05	0.97
		Inshore - offshore	<0.05	0.96
S_v of shallowest SSL	$S_{v,\ 1}$	Inshore - transition	<0.05	0.96
		Transition - offshore	<0.05	0.98
		Inshore - offshore	<0.05	0.93
Mean S_v of all SSLs	$S_{v,\ all}$	Inshore - transition	<0.05	0.97
		Transition - offshore	<0.05	0.92
		Inshore - offshore	<0.05	0.86
Number of SSLs	Ɒ	Inshore - transition	ns	–
		Transition - offshore	ns	–
		Inshore - offshore	ns	–
Minimal depth shallowest SSL	$đ_1$	Inshore - transition	ns	0.25
		Transition - offshore	ns	0.78
		Inshore - offshore	ns	ns
Width of shallowest SSL	$\dot{W}_1$	Inshore - transition	<0.05	0.94
		Transition - offshore	<0.05	0.83
		Inshore - offshore	<0.05	0.82
Vertical profiles of $S_{v,\ EI}$	n/a	Inshore - transition	<0.05	0.99
		Transition - offshore	ns	0.95
		Inshore - offshore	<0.05	0.96
$S_{v,\ EI}$ classes	n/a	Inshore - transition	ns	–
		Transition - offshore	ns	–
		Inshore - offshore	ns	–
Diel Vertical Migration Analyses (difference between daytime and nighttime)				
Mean S_v from echointegrated echograms $S_{v,\ EI}$	$S_{v,\ EI}$	Inshore - transition	ns	0.91
		Transition - offshore	ns	0.56
		Inshore - offshore	ns	0.12
S_v of shallowest SSL	$S_{v,\ 1}$	Inshore - transition	<0.05	0.47
		Transition - offshore	<0.05	0.78
		Inshore - offshore	<0.05	0.41
Mean S_v of all SSLs	$S_{v,\ all}$	Inshore - transition	<0.05	0.56
		Transition - offshore	<0.05	0.48
		Inshore - offshore	<0.05	−0.77
Number of SSLs	Ɒ	Inshore - transition	ns	–
		Transition - offshore	ns	–
		Inshore - offshore	ns	–
Minimal depth shallowest SSL	$đ_1$	Inshore - transition	<0.05	−0.13
		Transition - offshore	<0.05	0.83
		Inshore - offshore	ns	ns
Width of shallowest SSL	$\dot{W}_1$	Inshore - transition	<0.05	0.31
		Transition - offshore	ns	0.84
		Inshore - offshore	<0.05	0.24
Vertical profiles of $S_{v,\ EI}$	n/a	Inshore - transition	<0.05	−0.53
		Transition - offshore	<0.05	0.90
		Inshore - offshore	<0.05	−0.77

4.2. Diel vertical migration according to bathymetric areas

The majority of biomass involved in DVM comprises organisms larger than 1 mm, detected at 38 kHz (Hernández-León et al., 2001, 2007). Our study reveals distinct DVM behavioural differences between inshore and offshore areas, with intermediate signals observed in the transition area. The low correlation between inshore and transition areas likely stems from the divergence of signals around 45 m depth, possibly indicating different species compositions or DVM behaviours in inshore and offshore areas. At least three distinct pelagic communities are apparent: one inshore and two offshore. The positive difference in $đ_1$ between day and night suggests a variable behavioural response of organisms to depth availability and/or variability in species composition within the community.

The inshore community appears more compact during the night, located around 50 m, and more scattered during the daytime. This explains low pelagic biomass (S_v) values and aligns with DVM type I, as mostly reported in the Atlantic Ocean (Hays, 1996). Zooplankton species typically exhibit type I DVM, ascending to the surface during the night and descending to deeper layers during the day (Bianchi et al., 2013b; Cascão et al., 2019; Lehodey et al., 2015). The zooplankton community in the CCLME is dominated by copepods (Ariza et al., 2016), and clupeids and their larvae are part of the fish communities in the inshore area (Sarré et al., 2018; Tiedemann et al., 2017). The day-night difference could also be attributed to diel horizontal migrations, with organisms from all three bathymetric areas migrating to more coastal and shallower areas during the night (Benoit-Bird et al., 2001). This phenomenon may explain why pelagic biomass is consistently higher during the night than during the day. However, the difference in biomass could also be due to fish avoiding vessels more in shallow waters than in deeper areas (Brehmer et al., 2006).

Offshore, DVM indicates the presence of two distinct functional groups: one with positive tropism to light and the other with negative tropism. The highest pelagic biomass peak offshore is around 50 m depth during the night, demonstrating the formation of SSL in these areas during the night, unlike the inshore area. A portion of these communities migrates to the surface, and the majority migrates under 250 m depth, likely below the thermocline (Vélez-Bechi et al., 2015). The pelagic

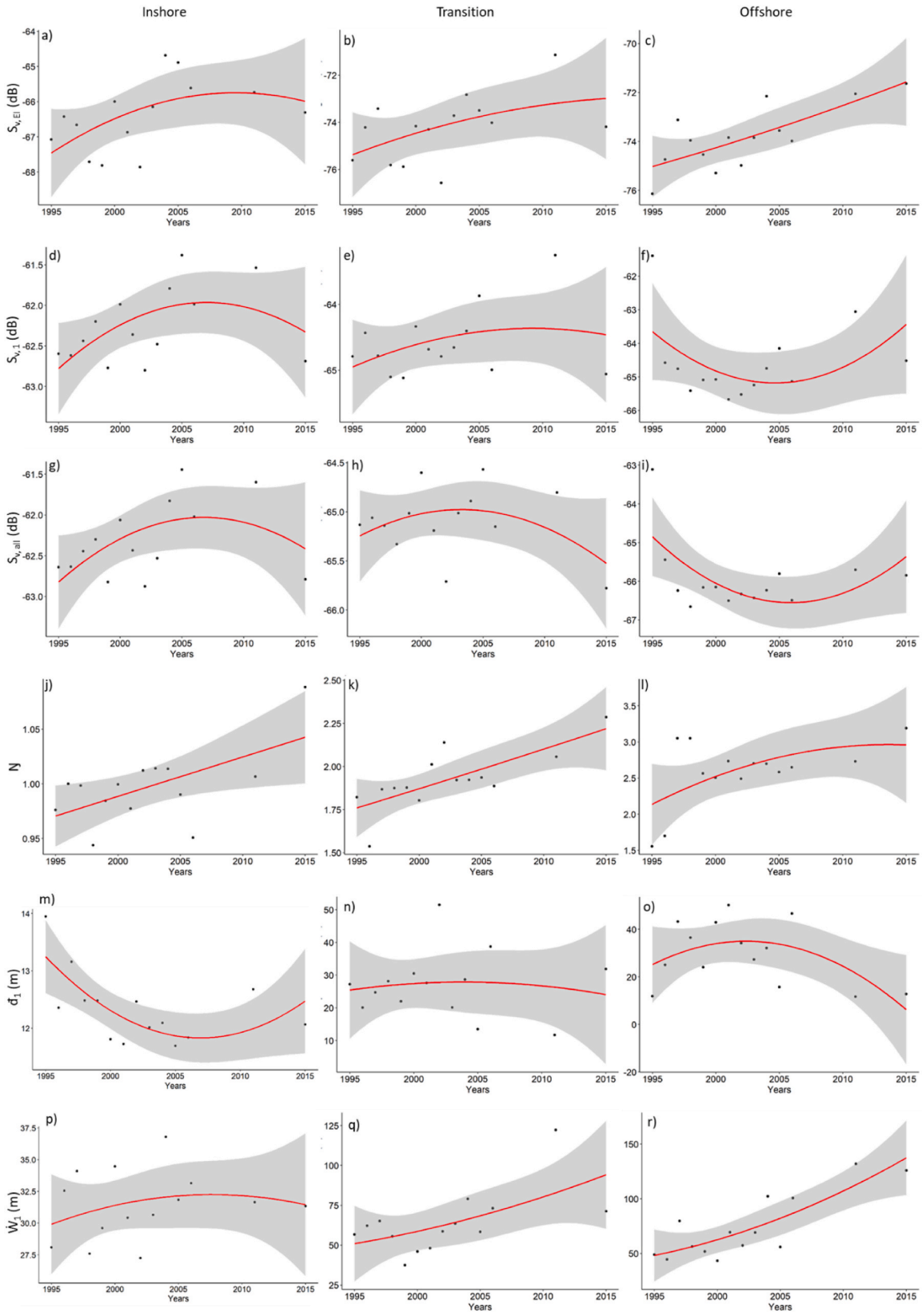

Fig. 8. Temporal patterns of acoustic descriptors surveyed over two decades (1995–2015) in different bathymetric areas. a - c) mean S_v from the whole water column ($S_{v,\ EI}$ in dB); d - f) mean S_v from the shallowest 'SSL' Sound Scattered Layer ($S_{v,1}$ in dB), and g - i) mean S_v from all SSLs ($S_{v,\ all}$ in dB); j - l) number of SSL (Ɒ); m - o) minimal depth of the shallowest SSL ($\dot{d}_1$ in m); p - r) width of shallowest SSL ($\dot{W}_1$ in m). First column a) d) g) j) m) p) represent the inshore area (bottom depth <150 m), the second b) e) h) k) n) q) the transition area (bottom depth in 150–500 m) and the third c) f) i) l) o) r) the offshore area (bottom depth >500 m). Red lines represent significant regression, either linear or polynomial. The grey shade represents the standard error.

Table 4
Regressions analysis results for sound scattering layers (SSLs) descriptors over the years (1995–2015). The polynomial order indicates the best regression ($p < 0.05$) calculated, ranging from 1 to 3. When the polynomial order is 1, the regression is linear. The estimate of first degree (E) represents the estimation of the first-order factor. The R^2 value indicated the adjusted R-squared.

Descriptor	Area		
	Inshore	Transition	Offshore
S_v from the whole water column ($S_{v,\ EI}$)	Order: 3 E: 201.54 $R^2 = 9.84\ 10^{-3}$	Order: 3 E: 154.70 $R^2 = 5.63\ 10^{-2}$	Order: 1 E: $1.58\ 10^{-2}$ $R^2 = 6.81\ 10^{-2}$
S_v from the shallowest SSL ($S_{v,\ 1}$)	Order: 3 E: 55.06 $R^2 = 5.84\ 10^{-3}$	Order: 3 E: 23.53 $R^2 = 1.73\ 10^{-2}$	Order: 3 E: 71.74 $R^2 = 5.82\ 10^{-2}$
S_v from all SSLs ($S_{v,\ all}$)	Order: 3 E: 49.45 $R^2 = 6.05\ 10^{-3}$	Order: 3 E: −22.21 $R^2 = 8.77\ 10^{-3}$	Order: 3 E: 17.07 $R^2 = 1.65\ 10^{-2}$
Number of SSLs (Ɒ)	Order: 1 E: $3.77\ 10^{-3}$ $R^2 = 2.35\ 10^{-3}$	Order: 1 E: $2.35\ 10^{-2}$ $R^2 = 1.66\ 10^{-2}$	Order: 3 E: 14.98 $R^2 = 1.20\ 10^{-2}$
Minimal depth of the shallowest SSL ($đ_1$)	Order: 3 E: −144.17 $R^2 = 5.38\ 10^{-3}$	Order: 3 E: non-significant $R^2 = 7.56\ 10^{-3}$	Order: 3 E: −1090.89 $R^2 = 1.43\ 10^{-2}$
Width of the shallowest SSL ($\dot{W}_1$)	Order: 3 E: 235.09 $R^2 = 9.71\ 10^{-4}$	Order: 3 E: 2616.86 $R^2 = 6.05\ 10^{-2}$	Order: 3 E: 3693.94 $R^2 = 6.17\ 10^{-2}$

biomass difference between night and day is positive from the surface to 250 m, indicating higher acoustic density with more organisms and/or denser communities. This difference is negative under 250 m depth, indicating that communities migrate from the upper part of the water column during the night to the lower part during the day. This type of DVM reflects a negative tropism to light. The most common fish larvae in the tropical Atlantic Ocean are myctophids (Dolar et al., 2003; Gushchin and Corten, 2017; Olivar et al., 2018) and microstomatids (Olivar et al., 2018). In the shallowest part of the water column (0–50 m), a part of the communities migrates to the surface during the daytime. These communities may be constituted by myctophid and microstomatid larvae, which only inhabit the upper zone (0–200 m). In deeper areas, larvae are not found. Therefore, a hypothesis is that myctophid and microstomatid larvae constitute a significant part of observed DVM, migrating from around 50 m during the night to deeper zones during the day. Around 500 m depth, we observe a low difference between day and night, reflecting the absence of DVM behavior in bathypelagic species. Three communities appear in the transition area, combining inshore (scattering during the night) and offshore (migrating to the surface and migrating deeper) characteristics.

DVM plays a crucial role in ecosystems, influencing trophic interactions (Pinti et al., 2021) and the carbon export flux of the biological pump (Archibald et al., 2019). Without biological sampling, species composition remains challenging to validate. Still, studies by Hernández-León et al. (2007) and Diogoul et al. (2021) suggest that the zooplankton composition is dominated by copepods in the SCCLME, with a high diversity of fish listed in the area (Ariza et al., 2016; Olivar et al., 2018). Nevertheless, the functioning can be described and is found to differ across the three bathymetric areas considered.

4.3. Inter-annual trends

The significant increase in the number of Sound Scattering Layers (SSLs) (Ɒ) and pelagic biomass ($S_{v,\ EI}$) across all bathymetric areas corresponds to the rise in sea surface temperature (Diogoul et al., 2021; Gómez-Letona et al., 2017) and increased upwelling intensity (Benazzouz et al., 2015) observed during the two decades studied, potentially linked to global climate change. These parameters have the potential to impact the marine food web and may explain the observed inter-annual trends. The increase in Ɒ may result from the fragmentation of existing SSLs. For surface SSLs, this fragmentation could be linked to the strong winds generated by upwelling in the region. However, other parameters should be explored, including physicochemical parameters (Diogoul et al., 2020) and species composition, as changes in species composition can influence SSL depth and dimensions. The significant increase in the width of the shallowest SSL ($\dot{W}_1$) observed in both transition and offshore areas suggests an increase in the size of these SSLs, indicating a probable increase in their pelagic biomass (Fig. S2).

The offshore area exhibited a distinct significant trend over the years, with $S_{v,\ EI}$ significantly increasing, a phenomenon not observed in other areas. Moreover, $S_{v,\ 1}$ from the shallowest SSL appeared to remain stable over the years. These results align with those of (Diogoul et al., 2021), suggesting that marine pelagic resources, mainly fish and plankton in the continental shelf of the SCCLME, have remained relatively stable over the last two decades. Therefore, the observed increase in pelagic biomass was not solely due to aggregated organisms in SSLs but encompassed the entire water column. Two possible explanations for this phenomenon warrant further exploration: changes in species composition or alterations in schooling behaviour (Brehmer et al., 2007).

Three parameters ($S_{v,\ 1}$, $S_{v,\ all}$, and $đ_1$) exhibited fluctuations along the time series, with alternating periods of increase and decrease, suggesting a cyclic phenomenon with a periodicity of approximately 10 years. These well-known cyclic patterns (*e.g.* Kawasaki, 1992; Bertrand et al., 2004) impact pelagic communities at the decadal scale. The fluctuations are attributed to organism life cycles (Kawasaki, 1992) and environmental factors such as ocean oscillations (Alexander et al., 2014; Knight et al., 2006). The multi-decadal oscillations of the Atlantic Ocean (Schlesinger and Ramankutty, 1994) have known impacts on ecosystem functioning (Edwards et al., 2013; Nye et al., 2014) and SSL structures (Hays et al., 2005). The long-term dataset in this study has highlighted the responses of SSLs, as indicated by pelagic biomass ($S_{v,\ 1}$ and $S_{v,\ all}$) and minimal depth ($đ_1$), to these cyclical ocean oscillations. For instance, the $S_{v,\ 1}$ in the inshore area displayed an increase from 1995 to 2005, followed by a decrease from 2005 to 2015, which is the same variation that heat content anomalies observed in the Atlantic over the past decades (NOAA PSL, 2023). Moreover, these oscillations are known to impact pelagic ecosystems, including fish and zooplankton (Alheit et al., 2014), which is observable in the SSLs.

This study highlights differences between three bathymetric areas: inshore (<150 m), transition (150–500 m) and offshore (>500 m). Several methodologies have been used to distinguish their functioning and vertical structuration, including diel vertical migrations. Inshore and transition present similarities, while offshore is quite different. Inter-annual trends can also be analyzed to highlight differences between ecosystems in the face of large-scale variations. Using only acoustic data allows large dataset with a non-intrusive and non-destructive tool. Furthermore, it underscores the need for targeted research and monitoring efforts that capture the complexity and heterogeneity of LMEs. However, acoustic only has limitation, as there is no information about species composition or environmental variables. Further analyses are in process to integrate other data, especially from satellites, and to attribute information about species using multi-frequencies.

5. Conclusion

By studying the effect of bathymetry on pelagic spatial organization, we found that SSL descriptors were effective in monitoring SSLs and pelagic micro-nektonic communities, and echointegration descriptors provided useful complementary information. We recommends using SSL

descriptors to monitor the non-specific spatial organization of pelagic communities in marine ecosystems. These findings have implications for future studies on the distribution and behaviour of marine organisms in LMEs. This information is useful for refining our understanding of the fine-scale spatial distribution of marine organisms and their habitat preferences.

Higher acoustic pelagic biomass was noted in shallower waters, revealing a distinct correlation between the vertical structure of the water column and the bathymetric area. These findings highlight the importance of considering separate bathymetric areas within LMEs as distinct communities exhibiting diverse spatial structures and DVM behaviours. Moreover, our results indicate the potential implications of these findings on various biological processes, such as the biological carbon pump and trophic interactions within such ecosystems. By acknowledging the variability between inshore and offshore areas, LME studies can better account for the unique characteristics and dynamics of each bathymetric area. This knowledge is essential for understanding and predicting ecosystem-level processes and for informing effective conservation and management strategies. Overall, our study sheds light on the intricate relationships between bathymetric areas, community dynamics, and key ecological processes. These findings emphasize the significance of incorporating spatial considerations into future LME studies and provide a foundation for further investigations into the functioning and resilience of these valuable marine ecosystems.

CRediT authorship contribution statement

Anne Mouget: Writing – original draft, Investigation, Formal analysis. **Patrice Brehmer:** Visualization, Validation, Supervision, Funding acquisition, Conceptualization. **Mohamed Ahmed Jeyid:** Validation. **Yannick Perrot:** Validation, Software, Methodology. **Ndague Diogoul:** Validation. **Momodou Sidibeh:** Validation. **Kamel Mamza:** Validation. **Anthony Acou:** Validation, Supervision. **Abdoulaye Sarré:** Validation, Resources, Data curation, Conceptualization.

Declaration of competing interest

The authors declare that they have no known competing financial interests or personal relationships that could have appeared to influence the work reported in this paper.

Acknowledgements

This work was done within the AWA "Ecosystem Approach to the management of fisheries and the marine environment in West African waters" project funded by IRD and the BMBF (grant 01DG12073E and 01DG12073B), www.awa.ird.fr (SRFC: Sub Regional Fisheries Commission) and the PREFACE project funded by the European Commission's Seventh Framework Program (2007–2013) under Grant Agreement number 603521, https://preface.b.uib.no/and ended within TriAtlas European project grant number 817578 and nextGEMS funded through the European Union's Horizon 2020 research and innovation program under the grant agreement number 101003470. We thank the Nansen project (FAO/IMR), Dr Jens-Otto Krakstad (IMR, Norway) as FAO, and African colleagues for data collection, particularly Salahedine El-Ayoubi (INRH, Morocco). This work has also been supported by ARED funding from the Brittany region (France). We thank Pr. Eric Feunteun (MNHN, France) for the advice and review as well as the IRD fisheries acoustics team (IUEM/UMR Lemar) in Plouzané (campus Ifremer, France).

Appendix A. Supplementary data

Supplementary data to this article can be found online at https://doi.org/10.1016/j.csr.2024.105372.

References

Aksnes, D.L., Røstad, A., Kaartvedt, S., Martinez, U., Duarte, C.M., Irigoien, X., 2017. Light penetration structures the deep acoustic scattering layers in the global ocean. Sci. Adv. 3, e1602468. https://doi.org/10.1126/sciadv.1602468.

Alexander, M.A., Halimeda Kilbourne, K., Nye, J.A., 2014. Climate variability during warm and cold phases of the Atlantic Multidecadal Oscillation (AMO) 1871–2008. J. Mar. Syst., Atlantic Multidecadal Oscillation-mechanism and impact on marine ecosystems 133, 14–26. https://doi.org/10.1016/j.jmarsys.2013.07.017.

Alheit, J., Licandro, P., Coombs, S., Garcia, A., Giráldez, A., Santamaría, M.T.G., Slotte, A., Tsikliras, A.C., 2014. Reprint of "Atlantic Multidecadal Oscillation (AMO) modulates dynamics of small pelagic fishes and ecosystem regime shifts in the eastern North and Central Atlantic.". J. Mar. Syst., Atlantic Multidecadal Oscillation-mechanism and impact on marine ecosystems 133, 88–102. https://doi.org/10.1016/j.jmarsys.2014.02.005.

Archibald, K.M., Siegel, D.A., Doney, S.C., 2019. Modeling the impact of zooplankton diel vertical migration on the carbon export flux of the biological pump. Global Biogeochem. Cycles 33, 181–199. https://doi.org/10.1029/2018GB005983.

Arístegui, J., Barton, E.D., Álvarez-Salgado, X.A., Santos, A.M.P., Figueiras, F.G., Kifani, S., Hernández-León, S., Mason, E., Machú, E., Demarcq, H., 2009. Sub-regional ecosystem variability in the Canary Current upwelling. Prog. Oceanogr., Eastern Boundary Upwelling Ecosystems: Integrative and Comparative Approaches 83, 33–48. https://doi.org/10.1016/j.pocean.2009.07.031.

Ariza, A., Landeira, J.M., Escánez, A., Wienerroither, R., Aguilar de Soto, N., Røstad, A., Kaartvedt, S., Hernández-León, S., 2016. Vertical distribution, composition and migratory patterns of acoustic scattering layers in the Canary Islands. J. Mar. Syst. 157, 82–91. https://doi.org/10.1016/j.jmarsys.2016.01.004.

Ariza, A., Lengaigne, M., Menkes, C., Lebourges-Dhaussy, A., Receveur, A., Gorgues, T., Habasque, J., Gutiérrez, M., Maury, O., Bertrand, A., 2022. Global decline of pelagic fauna in a warmer ocean. Nat. Clim. Change 12, 928–934. https://doi.org/10.1038/s41558-022-01479-2.

Auger, P.-A., Gorgues, T., Machu, E., Aumont, O., Brehmer, P., 2016. What drives the spatial variability of primary productivity and matter fluxes in the north-west African upwelling system? A modelling approach. Biogeosciences 13, 6419–6440. https://doi.org/10.5194/bg-13-6419-2016.

Barton, E.D., Arístegui, J., Tett, P., Cantón, M., García-Braun, J., Hernández-León, S., Nykjaer, L., Almeida, C., Almunia, J., Ballesteros, S., Basterretxea, G., Escánez, J., García-Weill, L., Hernández-Guerra, A., López-Laatzen, F., Molina, R., Montero, M. F., Navarro-Pérez, E., Rodríguez, J.M., van Lenning, K., Vélez, H., Wild, K., 1998. The transition zone of the Canary Current upwelling region. Prog. Oceanogr. 41, 455–504. https://doi.org/10.1016/S0079-6611(98)00023-8.

Barton, E.D., Field, D.B., Roy, C., 2013. Canary current upwelling: more or less? Prog. Oceanogr. 116, 167–178. https://doi.org/10.1016/j.pocean.2013.07.007.

Beaugrand, G., Ibañez, F., Reid, P.C., 2000. Spatial, seasonal and long-term fluctuations of plankton in relation to hydroclimatic features in the English Channel, Celtic Sea and Bay of Biscay. Mar. Ecol. Prog. Ser. 200, 93–102. https://doi.org/10.3354/meps200093.

Béhagle, N., Cotté, C., Lebourges-Dhaussy, A., Roudaut, G., Duhamel, G., Brehmer, P., Josse, E., Cherel, Y., 2017. Acoustic distribution of discriminated micronektonic organisms from a bi-frequency processing: the case study of eastern Kerguelen oceanic waters. Prog. Oceanogr. 156, 276–289. https://doi.org/10.1016/j.pocean.2017.06.004.

Béhagle, N., Cotté, C., Ryan, T.E., Gauthier, O., Roudaut, G., Brehmer, P., Josse, E., Cherel, Y., 2016. Acoustic micronektonic distribution is structured by macroscale oceanographic processes across 20–50°S latitudes in the South-Western Indian Ocean. Deep-Sea Res. Part A Oceanogr. Res. Pap. 110, 20–32. https://doi.org/10.1016/j.dsr.2015.12.007.

Béhagle, N., du Buisson, L., Josse, E., Lebourges-Dhaussy, A., Roudaut, G., Ménard, F., 2014. Mesoscale features and micronekton in the Mozambique Channel: an acoustic approach. Deep Sea Res. Part II Top. Stud. Oceanogr., The Mozambique Channel: Mesoscale Dynamics and Ecosystem Responses 100, 164–173. https://doi.org/10.1016/j.dsr2.2013.10.024.

Benazzouz, A., Demarcq, H., González-Nuevo, G., 2015. Recent changes and trends of the upwelling intensity in the canary current large marine ecosystem. In: Valdés, L., Déniz-Gonzalez, I. (Eds.), Oceanographic and Biological Features in the Canary Current Large Marine Ecosystem. IOC-UNESCO, Paris, pp. 321–330.

Benazzouz, A., Mordane, S., Orbi, A., Chagdali, M., Hilmi, K., Atillah, A., Lluís Pelegrí, J., Hervé, D., 2014. An improved coastal upwelling index from sea surface temperature using satellite-based approach – the case of the Canary Current upwelling system. Continent. Shelf Res. 81, 38–54. https://doi.org/10.1016/j.csr.2014.03.012.

Benoit-Bird, K., Au, W., Brainard, R., Lammers, M., 2001. Diel horizontal migration of the Hawaiian mesopelagic boundary community observed acoustically. Mar. Ecol. Prog. Ser. 217, 1–14. https://doi.org/10.3354/meps217001.

Benoit-Bird, K.J., Au, W.W.L., 2004. Diel migration dynamics of an island-associated sound-scattering layer. Deep-Sea Res. Part A Oceanogr. Res. Pap. 51, 707–719. https://doi.org/10.1016/j.dsr.2004.01.004.

Bertrand, A., Misselis, C., Josse, E., Bach, P., 2000. Caractérisation hydrologique et acoustique de l'habitat pélagique en Polynésie française : conséquences sur les distributions horizontale et verticale des thonidés. In: Gascuel, D., Biseau, A., Bez, N., Chavance, Paris, P. (Eds.), Les Espaces de l'Halieutique, Actes Du Quatrième Forum Halieumétrique. Presented at the Coll. colloques et séminaires, pp. 55–74.

Bertrand, A., Segura, M., Gutierrez, M., Vasquez, L., 2004. From small-scale habitat loopholes to decadal cycles: a habitat-based hypothesis explaining fluctuation in pelagic fish populations off Peru. Fish Fish. 5, 296–316. https://doi.org/10.1111/j.1467-2679.2004.00165.x.

Bianchi, D., Stock, C., Galbraith, E.D., Sarmiento, J.L., 2013a. Diel vertical migration: ecological controls and impacts on the biological pump in a one-dimensional ocean model. Global Biogeochem. Cycles 27, 478–491. https://doi.org/10.1002/gbc.20031.

Bianchi, D., Stock, C., Galbraith, E.D., Sarmiento, J.L., 2013b. Diel vertical migration: ecological controls and impacts on the biological pump in a one-dimensional ocean model: diel vertical migration impacts. Global Biogeochem. Cycles 27, 478–491. https://doi.org/10.1002/gbc.20031.

Blanluet, A., Doray, M., Berger, L., Romagnan, J.-B., Le Bouffant, N., Lehuta, S., Petitgas, P., 2019. Characterization of sound scattering layers in the Bay of Biscay using broadband acoustics, nets and video. PLoS One 14. https://doi.org/10.1371/journal.pone.0223618.

Brehmer, P., Gerlotto, F., Laurent, C., Cotel, P., Achury, A., Samb, B., 2007. Schooling behaviour of small pelagic fish: phenotypic expression of independent stimuli. Mar. Ecol. Prog. Ser. 334, 263–272. https://doi.org/10.3354/meps334263.

Brehmer, P., Guillard, J., Guennégan, Y., Bigot, J.L., Liorzou, B., 2006. Evidence of a variable "unsampled" pelagic fish biomass in shallow water (<20 m): the case of the Gulf of Lion. ICES J. Mar. Sci. 63, 444–451. https://doi.org/10.1016/j.icesjms.2005.10.016.

Brehmer, P., Sancho, G., Trygonis, V., Itano, D., Dalen, J., Fuchs, A., Faraj, A., Taquet, M., 2019. Towards an autonomous pelagic observatory: experiences from monitoring fish communities around drifting FADs. Thalass. Int. J. Mar. Sci. 35, 177–189. https://doi.org/10.1007/s41208-018-0107-9.

Brehmer, P.A.J.-P., 2006. Fisheries acoustics: theory and practice. Fish Fish. 7, 227–228. https://doi.org/10.1111/j.1467-2979.2006.00220.x, 2nd edn.

Brierley, A.S., 2014. Diel vertical migration. Curr. Biol. 24, R1074–R1076. https://doi.org/10.1016/j.cub.2014.08.054.

Brunel, T., Boucher, J., 2007. Long-term trends in fish recruitment in the north-east Atlantic related to climate change. Fish. Oceanogr. 16, 336–349. https://doi.org/10.1111/j.1365-2419.2007.00435.x.

Cade, D.E., Benoit-Bird, K.J., 2014. An automatic and quantitative approach to the detection and tracking of acoustic scattering layers. Limnol Oceanogr. Methods 12, 742–756. https://doi.org/10.4319/lom.2014.12.742.

Cascão, I., Domokos, R., Lammers, M.O., Santos, R.S., Silva, M.A., 2019. Seamount effects on the diel vertical migration and spatial structure of micronekton. Prog. Oceanogr. 175, 1–13. https://doi.org/10.1016/j.pocean.2019.03.008.

Castillo, S., Ramil, F., Ramos, A., 2017. Composition and distribution of epibenthic and demersal assemblages in Mauritanian deep-waters. In: Ramos, A., Ramil, F., Sanz, J. L. (Eds.), Deep-Sea Ecosystems off Mauritania: Research of Marine Biodiversity and Habitats in the Northwest African Margin. Springer, Netherlands, Dordrecht, pp. 317–353. https://doi.org/10.1007/978-94-024-1023-5_8.

Champalbert, G., Pagano, M., Kouamé, B., Riandey, V., 2005. Zooplankton spatial and temporal distribution in a tropical oceanic area off West Africa. Hydrobiologia 548, 251–265. https://doi.org/10.1007/s10750-005-5194-y.

Collins, M.A., Stowasser, G., Fielding, S., Shreeve, R., Xavier, J.C., Venables, H.J., Enderlein, P., Cherel, Y., Van de Putte, A., 2012. Latitudinal and bathymetric patterns in the distribution and abundance of mesopelagic fish in the Scotia Sea. Deep Sea Res. Part II Top. Stud. Oceanogr., DISCOVERY 2010: Spatial and Temporal Variability in a Dynamic Polar Ecosystem 59–60, 189–198. https://doi.org/10.1016/j.dsr2.2011.07.003.

Croux, C., Dehon, C., 2010. Influence functions of the Spearman and Kendall correlation measures. Stat. Methods Appl. 19, 497–515. https://doi.org/10.1007/s10260-010-0142-z.

David, V., Mouget, A., Perrot, Y., Le Goff, L., Thiriet, P., Diogoul, N., Feunteun, E., Acou, A., Brehmer, P., 2022. Insights from a multibeam echosounder to survey pelagic fish shoals and their spatio-temporal distribution in ultra-shallow waters. Estuar. Coast Shelf Sci. 264, 107705. https://doi.org/10.1016/j.ecss.2021.107705.

David, V., Mouget, A., Thiriet, P., Minart, C., Perrot, Y., Le Goff, L., Bianchimani, O., Basthard-Bogain, S., Estaque, T., Richaume, J., Sys, J.-F., Cheminée, A., Feunteun, E., Acou, A., Brehmer, P., 2024. Species identification of fish shoals using coupled split-beam and multibeam echosounders and two scuba-diving observational methods. J. Mar. Syst. 241, 103905. https://doi.org/10.1016/j.jmarsys.2023.103905.

De Robertis, A., Higginbottom, I., 2007. A post-processing technique to estimate the signal-to-noise ratio and remove echosounder background noise. ICES J. Mar. Sci. 64, 1282–1291. https://doi.org/10.1093/icesjms/fsm112.

Diankha, O., Demarcq, H., Fall, M., Thiao, D., Thiaw, M., Sow, B.A., Gaye, A.T., Brehmer, P., 2017. Studying the contribution of different fishing gears to the *Sardinella* small-scale fishery in Senegalese waters. Aquat. Living Resour. 30, 27. https://doi.org/10.1051/alr/2017027.

Diogoul, N., Brehmer, P., Demarcq, H., El Ayoubi, S., Thiam, A., Sarre, A., Mouget, A., Perrot, Y., 2021. On the robustness of an eastern boundary upwelling ecosystem exposed to multiple stressors. Sci. Rep. 11, 12. https://doi.org/10.1038/s41598-021-81549-1.

Diogoul, N., Brehmer, P., Kiko, R., Perrot, Y., Lebourges-Dhaussy, A., Rodrigues, E., Thiam, A., Mouget, A., Ayoubi, S.E., Sarré, A., 2024. Estimating the copepod biomass in the North West African upwelling system using a bi-frequency acoustic approach. PLoS One 19, e0308083. https://doi.org/10.1371/journal.pone.0308083.

Diogoul, N., Brehmer, P., Perrot, Y., Tiedemann, M., Thiam, A., El Ayoubi, S., Mouget, A., Migayrou, C., Sadio, O., Sarré, A., 2020. Fine-scale vertical structure of sound-scattering layers over an east border upwelling system and its relationship to pelagic habitat characteristics. Ocean Sci. 16, 65–81. https://doi.org/10.5194/os-16-65-2020.

Dolar, M.L.L., Walker, W.A., Kooyman, G.L., Perrin, W.F., 2003. Comparative feeding ecology of spinner dolphins (STENELLA longirostris) and FRASER'S dolphins (lagenodelphis hosei) in the sulu sea. Mar. Mamm. Sci. 19, 1–19. https://doi.org/10.1111/j.1748-7692.2003.tb01089.x.

Domokos, R., 2009. Environmental effects on forage and longline fishery performance for albacore (Thunnus alalunga) in the American Samoa Exclusive Economic Zone. Fish. Oceanogr. 18, 419–438. https://doi.org/10.1111/j.1365-2419.2009.00521.x.

Edwards, M., Beaugrand, G., Helaouët, P., Alheit, J., Coombs, S., 2013. Marine ecosystem response to the atlantic multidecadal oscillation. PLoS One 8, e57212. https://doi.org/10.1371/journal.pone.0057212.

Fay, M.P., Proschan, M.A., 2010. Wilcoxon-Mann-Whitney or t-test? On assumptions for hypothesis tests and multiple interpretations of decision rules. Stat. Surv. 4, 1–39. https://doi.org/10.1214/09-SS051.

Faye, S., Lazar, A., Sow, B., Gaye, A., 2015. A model study of the seasonality of sea surface temperature and circulation in the Atlantic North-eastern Tropical Upwelling System. Front. Physiol. 3.

Foote, K.G., Knudsen, H.P., Vestnes, G., MacLennan, D.N., Simmonds, E.J., 1987. Calibration of Acoustic Instruments for Fish Density Estimation : a Practical Guide (Technical Report No. 144). ICES Cooperative.

Gasol, J.M., del Giorgio, P.A., Duarte, C.M., 1997. Biomass distribution in marine planktonic communities. Am. Soc. Limnol. Oceanogr. 42, 1353–1363.

Zonation of deep biota on continental margins. In: Gibson, R.N., Atkinson, R.J.A., Gordon, J.D.M. (Eds.), 2005. Oceanography and Marine Biology. CRC Press, pp. 221–288. https://doi.org/10.1201/9781420037449-8.

Gómez-Letona, M., Ramos, A.G., Coca, J., Arístegui, J., 2017. Trends in primary production in the canary current upwelling system—a regional perspective comparing remote sensing models. Front. Mar. Sci. 4.

Görlitz, S., Interwies, E., 2013. Protection of the Canary Current Large Marine Ecosystem (CCLME) - Economic and Social Valuation of the CCLME Ecosystem Services.

Guglielmo, L., Minutoli, R., Bergamasco, A., Granata, A., Zagami, G., Antezana, T., 2011. Short-term changes in zooplankton community in Paso Ancho basin (Strait of Magellan): functional trophic structure and diel vertical migration. Polar Biol. 34, 1301–1317. https://doi.org/10.1007/s00300-011-1031-0.

Gushchin, A.V., Corten, A., 2017. Feeding of pelagic fish in waters of Mauritania: 3.—atlantic Chub mackerel Scomber colias, Atlantic horse mackerel Trachurus trachurus, Cunene horse mackerel Trachurus trecae. J. Ichthyol. 57, 410–423. https://doi.org/10.1134/S0032945217030067.

Hays, G.C., 1996. Large-scale patterns of diel vertical migration in the North Atlantic. Deep-Sea Res. Part A Oceanogr. Res. Pap. 43, 1601–1615. https://doi.org/10.1016/S0967-0637(96)00078-7.

Hays, G.C., Richardson, A.J., Robinson, C., 2005. Climate change and marine plankton. Trends Ecol. Evol., SPECIAL ISSUE: BUMPER BOOK REVIEW 20, 337–344. https://doi.org/10.1016/j.tree.2005.03.004.

Hazen, E.L., Johnston, D.W., 2010. Meridional patterns in the deep scattering layers and top predator distribution in the central equatorial Pacific. Fish. Oceanogr. 19, 427–433. https://doi.org/10.1111/j.1365-2419.2010.00561.x.

Hedger, R., McKenzie, E., Heath, M., Wright, P., Scott, B., Gallego, A., Andrews, J., 2004. Analysis of the spatial distributions of mature cod (Gadus morhua) and haddock (Melanogrammus aeglefinus) abundance in the North Sea (1980–1999) using generalised additive models. Fish. Res. 70, 17–25. https://doi.org/10.1016/j.fishres.2004.07.002.

Hernández-León, S., Gómez, M., Arístegui, J., 2007. Mesozooplankton in the Canary Current System: the coastal–ocean transition zone. Prog. Oceanogr., Ecological Functioning of the Iberian Seas: A synthesis of GLOBEC Research in Spain and Portugal 74, 397–421. https://doi.org/10.1016/j.pocean.2007.04.010.

Hernández-León, S., Gómez, M., Pagazaurtundua, M., Portillo-Hahnefeld, A., Montero, I., Almeida, C., 2001. Vertical distribution of zooplankton in Canary Island waters: implications for export flux. Deep-Sea Res. Part A Oceanogr. Res. Pap. 48, 1071–1092. https://doi.org/10.1016/S0967-0637(00)00074-1.

Hersey, J.B., Backus, R.H., Hellwig, J., 1961. Sound-scattering spectra of deep scattering layers in the western North Atlantic Ocean. Deep Sea Res. 8, 196–210. https://doi.org/10.1016/0146-6313(61)90021-1, 1953.

Holland, M.M., Becker, A., Smith, J.A., Everett, J.D., Suthers, I.M., 2021. Characterizing the three-dimensional distribution of schooling reef fish with a portable multibeam echosounder. Limnol Oceanogr. Methods 19, 340–355. https://doi.org/10.1002/lom3.10427.

Huan, Y., Sun, D., Wang, S., Zhang, H., Li, Z., He, Y., 2022. Phytoplankton size classes in the global ocean at different bathymetric depths. IEEE Trans. Geosci. Rem. Sens. 60, 1–11. https://doi.org/10.1109/TGRS.2022.3153477.

Ifremer, 2024. MOVIES3D.

Jones, I.S.F., Xie, J., 1994. A sound scattering layer in a freshwater reservoir. Limnol. Oceanogr. 39, 443–448. https://doi.org/10.4319/lo.1994.39.2.0443.

Kaschner, K., Watson, R., Trites, A.W., Pauly, D., 2006. Mapping world-wide distributions of marine mammal species using a relative environmental suitability (RES) model. Mar. Ecol. Prog. Ser. 316, 285–310. https://doi.org/10.3354/meps316285.

Kawasaki, T., 1992. Mechanisms governing fluctuations in pelagic fish populations. South Afr. J. Mar. Sci. 12, 873–879. https://doi.org/10.2989/02577619209504748.

Knight, J.R., Folland, C.K., Scaife, A.A., 2006. Climate impacts of the atlantic multidecadal oscillation. Geophys. Res. Lett. 33. https://doi.org/10.1029/2006GL026242.

Lehodey, P., Conchon, A., Senina, I., Domokos, R., Calmettes, B., Jouanno, J., Hernandez, O., Kloser, R., 2015. Optimization of a micronekton model with acoustic data. ICES J. Mar. Sci. 72, 1399–1412. https://doi.org/10.1093/icesjms/fsu233.

Lenoir, S., Beaugrand, G., Lecuyer, É., 2011. Modelled spatial distribution of marine fish and projected modifications in the North Atlantic Ocean. Global Change Biol. 17, 115–129. https://doi.org/10.1111/j.1365-2486.2010.02229.x.

Louisy, P., 2015. Guide d'identification des poissons marins: Europe et Méditerranée, 3e éd. entièrement revue. complétée et mise à jour. Ulmer, Paris.

MacLennan, D.N., Fernandes, P.G., Dalen, J., 2002. A consistent approach to definitions and symbols in fisheries acoustics. ICES J. Mar. Sci. 59, 365–369. https://doi.org/10.1006/jmsc.2001.1158.
Macpherson, E., Duarte, C.M., 1991. Bathymetric trends in demersal fish size: is there a general relationship? Mar. Ecol. Prog. Ser. 71, 103–112.
Majewski, A.R., Atchison, S., MacPhee, S., Eert, J., Niemi, A., Michel, C., Reist, J.D., 2017. Marine fish community structure and habitat associations on the Canadian Beaufort shelf and slope. Deep-Sea Res. Part A Oceanogr. Res. Pap. 121, 169–182. https://doi.org/10.1016/j.dsr.2017.01.009.
Maravelias, C.D., 1999. Habitat selection and clustering of a pelagic fish: effects of topography and bathymetry on species dynamics. Can. J. Fish. Aquat. Sci. 56, 437–450. https://doi.org/10.1139/f98-176.
Marchal, E., Gerlotto, F., Stequert, B., 1993. On the relationship between scattering layer, thermal structure and tuna abundance in the eastern atlantic equatorial current system. Oceanol. Acta 16, 261–272.
Mbaye, B.C., Brochier, T., Echevin, V., Lazar, A., Lévy, M., Mason, E., Gaye, A.T., Machu, E., 2015. Do Sardinella aurita spawning seasons match local retention patterns in the Senegalese–Mauritanian upwelling region? Fish. Oceanogr. 24, 69–89. https://doi.org/10.1111/fog.12094.
McHugh, M.L., 2013. The Chi-square test of independence. Biochem. Medica Biochem. Medica 23, 143–149. https://doi.org/10.11613/BM.2013.018.
Mouget, A., Brehmer, P., Perrot, Y., Uanivi, U., Diogoul, N., El Ayoubi, S., Jeyid, M.A., Sarré, A., Béhagle, N., Kouassi, A.M., Feunteun, E., 2022. Applying acoustic scattering layer descriptors to depict mid-trophic pelagic organisation: the case of Atlantic African large marine ecosystems continental shelf. Fishes 7, 86. https://doi.org/10.3390/fishes7020086.
Netburn, A.N., Koslow, J.A., 2015. Dissolved oxygen as a constraint on daytime deep scattering layer depth in the southern California current ecosystem. Deep Sea Res. Part Oceanogr. Res. Pap. 104, 149–158. https://doi.org/10.1016/j.dsr.2015.06.006.
NOAA PSL, 2023. Kaplan Extanded SST V2, Data provided by the NOAA PSL. Boulder, Colorado.
Nye, J.A., Baker, M.R., Bell, R., Kenny, A., Kilbourne, K.H., Friedland, K.D., Martino, E., Stachura, M.M., Van Houtan, K.S., Wood, R., 2014. Ecosystem effects of the atlantic multidecadal oscillation. J. Mar. Syst., Atlantic Multidecadal Oscillation-mechanism and impact on marine ecosystems 133, 103–116. https://doi.org/10.1016/j.jmarsys.2013.02.006.
Olivar, M.P., Contreras, T., Hulley, P.A., Emelianov, M., López-Pérez, C., Tuset, V., Castellón, A., 2018. Variation in the diel vertical distributions of larvae and transforming stages of oceanic fishes across the tropical and equatorial Atlantic. Prog. Oceanogr. 160, 83–100. https://doi.org/10.1016/j.pocean.2017.12.005.
Perrot, Y., Brehmer, P., Habasque, J., Roudaut, G., Behagle, N., Sarré, A., Lebourges-Dhaussy, A., 2018. Matecho: an open-source tool for processing fisheries acoustics data. Acoust Aust. https://doi.org/10.1007/s40857-018-0135-x.
Pinti, J., Andersen, K.H., Visser, A.W., 2021. Co-adaptive behavior of interacting populations in a habitat selection game significantly impacts ecosystem functions. J. Theor. Biol. 523, 110663. https://doi.org/10.1016/j.jtbi.2021.110663.
Proud, R., Cox, M.J., Wotherspoon, S., Brierley, A.S., 2015. A method for identifying Sound Scattering Layers and extracting key characteristics. Methods Ecol. Evol. 6, 1190–1198. https://doi.org/10.1111/2041-210X.12396.
R Core Team, 2021. R: A Language and Environment for Statistical Computing.
Remond, B., 2015. Les couches diffusantes du golfe de Gascogne : caractérisation acoustique, composition spécifique et distribution spatiale.
Sabarros, P.S., Ménard, F., Lévénez, P., Tew-Kai, P., Ternon, J.F., 2009. Mesoscale eddies influence distribution and aggregation patterns of micronekton in the Mozambique Channel. Mar. Ecol. Prog. Ser. 395, 101–107.
Sarré, A., Demarcq, H., Keenlyside, N., Krakstad, J.-O., El Ayoubi, S., Jeyid, A.M., Faye, S., Mbaye, A., Sidibeh, M., Brehmer, P., 2024. Climate change impacts on small pelagic fish distribution in Northwest Africa: trends, shifts, and risk for food security. Sci. Rep. 14, 12684. https://doi.org/10.1038/s41598-024-61734-8.
Sarré, A., Krakstad, J.-O., Brehmer, P., Mbye, E.M., 2018. Spatial distribution of main clupeid species in relation to acoustic assessment surveys in the continental shelves of Senegal and the Gambia. Aquat. Living Resour. 31, 9. https://doi.org/10.1051/alr/2017049.
Schalk, P.H., 1988. Observations on sound scattering layers in the upwelling off N.W. Africa and in the North equatorial current. J. Plankton Res. 10, 89–100. https://doi.org/10.1093/plankt/10.1.89.
Schickele, A., Leroy, B., Beaugrand, G., Goberville, E., Hattab, T., Francour, P., Raybaud, V., 2020. Modelling European small pelagic fish distribution: methodological insights. Ecol. Model. 416, 108902. https://doi.org/10.1016/j.ecolmodel.2019.108902.
Schlesinger, M.E., Ramankutty, N., 1994. An oscillation in the global climate system of period 65–70 years. Nature 367, 723–726.
Sheather, S.J., Jones, M.C., 1991. A reliable data-based bandwidth selection method for kernel density estimation. J. R. Stat. Soc. Ser. B Methodol. 53, 683–690.
Sherman, K., 1994. Sustainability, biomass yields, and health of coastal ecosystems: an ecological perspective. Mar. Ecol. Prog. Ser., Marine Ecology Progress Series 112, 277–301.
Simmonds, E.J., MacLennan, D.N., 2005. Fisheries acoustics: theory and practice. Fish and Aquatic Resources Series, second ed. Blackwell Science, Oxford ; Ames, Iowa.
Smith, K.F., Brown, J.H., 2002. Patterns of diversity, depth range and body size among pelagic fishes along a gradient of depth. Global Ecol. Biogeogr. 11, 313–322. https://doi.org/10.1046/j.1466-822X.2002.00286.x.
Spall, M.A., 1990. Circulation in the Canary Basin: a model/data analysis. J. Geophys. Res. Oceans 95, 9611–9628. https://doi.org/10.1029/JC095iC06p09611.
Tiedemann, M., Brehmer, P., 2017. Larval fish assemblages across an upwelling front: indication for active and passive retention. Estuar. Coast Shelf Sci. 187, 118–133. https://doi.org/10.1016/j.ecss.2016.12.015.
Tiedemann, M., Fock, H.O., Brehmer, P., Döring, J., Möllmann, C., 2017. Does upwelling intensity determine larval fish habitats in upwelling ecosystems? The case of Senegal and Mauritania. Fish. Oceanogr. 26, 655–667. https://doi.org/10.1111/fog.12224.
Urmy, S.S., Horne, J.K., Barbee, D.H., 2012. Measuring the vertical distributional variability of pelagic fauna in Monterey Bay. ICES J. Mar. Sci. 69, 184–196. https://doi.org/10.1093/icesjms/fsr205.
Vélez-Bechi, P., Gonzalez-Carballo, M., Pérez-Hernandez, M.D., Hernandez-Guerra, A., 2015. Open ocean temperature and salinity trends in the canary current large marine ecosystem. IOC Tech. Ser. Oceanographic and Biological Features in the Canary Current Large Marine Ecosystem, pp. 299–309.
Weill, A., Scalabrin, C., Diner, N., 1993. MOVIES-B: an acoustic detection description software. Application to shoal species' classification. Aquat. Living Resour. 6, 255–267. https://doi.org/10.1051/alr:1993026.
Weston, D.E., 1958. Observations on a scattering layer at the thermocline. Deep Sea Res. 5, 44–50. https://doi.org/10.1016/S0146-6291(58)80007-7, 1953.
Woillez, M., Poulard, J.-C., Rivoirard, J., Petitgas, P., Bez, N., 2007. Indices for capturing spatial patterns and their evolution in time, with application to European hake (Merluccius merluccius) in the Bay of Biscay. ICES J. Mar. Sci. 64, 537–550. https://doi.org/10.1093/icesjms/fsm025.
Zhang, G., Zhu, A.-X., Windels, S.K., Qin, C.-Z., 2018. Modelling species habitat suitability from presence-only data using kernel density estimation. Ecol. Indicat. 93, 387–396. https://doi.org/10.1016/j.ecolind.2018.04.002.